Bioorganic & Medicinal Chemistry xxx (2014) xxx–xxx

Contents lists available at ScienceDirect

Bioorganic & Medicinal Chemistry

journal homepage: www.elsevier.com/locate/bmc

Pyrrole-3-carboxamides as potent and selective JAK2 inhibitors

Maria Gabriella Brasca *, Marcella Nesi, Nilla Avanzi, Dario Ballinari, Tiziano Bandiera, Jay Bertrand, Simona Bindi, Giulia Canevari, Davide Carenzi, Daniele Casero, Lucio Ceriani, Marina Ciomei, Alessandra Cirla, Maristella Colombo, Sabrina Cribioli, Cinzia Cristiani, Franco Della Vedova, Gabriele Fachin, Marina Fasolini, Eduard R. Felder, Arturo Galvani, Antonella Isacchi, Danilo Mirizzi, Ilaria Motto, Achille Panzeri, Enrico Pesenti, Paola Vianello, Paola Gnocchi, Daniele Donati

Nerviano Medical Sciences S.r.l., Oncology, Viale Pasteur 10, 20014 Nerviano (MI), Italy

ARTICLE INFO

Article history:
Received 6 May 2014
Revised 11 June 2014
Accepted 12 June 2014
Available online xxxx

Keywords:
JAK2
Myeloproliferative disorders
Protein kinase inhibitor
Tumour cell proliferation inhibition
Anti-cancer agents

ABSTRACT

We report herein the discovery, structure guided design, synthesis and biological evaluation of a novel class of JAK2 inhibitors. Optimization of the series led to the identification of the potent and orally bioavailable JAK2 inhibitor **28** (NMS-P953). Compound **28** displayed significant tumour growth inhibition in SET-2 xenograft tumour model, with a mechanism of action confirmed in vivo by typical modulation of known biomarkers, and with a favourable pharmacokinetic and safety profile.

1. Introduction

JAK2 is a member of the Janus kinase (JAK) family of intracellular tyrosine kinases, which also include JAK1, JAK3 and TYK2. The JAK kinases are involved in signal transduction pathways mediated by cytokines, JAK2 in particular is a critical mediator for hormone-like cytokines such as growth hormone (GH), prolactin (PRL), erythropoietin (EPO), thrombopoietin (TPO), and cytokine receptor ligands involved in hematopoietic cell development, such as interleukin-3 (IL-3) or granulocyte-macrophage colony-stimulating factor (GM-CSF).[1] Moreover, deletion of JAK2 in mice resulted in embryonic lethality by day 12.5 (E12.5) due to a lack of hematopoiesis.[2,3] Upon ligand binding, JAKs phosphorylate tyrosine residues in the receptor cytoplasmic domains and in JAKs themselves leading to recruitment and activation of downstream signaling proteins such as signal transducer and activator of transcription (STAT). STAT phosphorylation leads to their dimerization and translocation to the nucleus where they regulate expression of specific genes involved in proliferation, apoptosis and differentiation.[4] Recently, a non canonical nuclear action of JAK1 and JAK2 has been described to affect gene expression by activating other transcription factors besides the STATs and exerting epigenetic actions, for example, by phosphorylating histone H3.[5] The Janus kinases are characterized by 7 distinct JAK homology regions (JH1 to JH7). The catalytically active kinase domain (JH1) is located at the carboxy-terminus, immediately adjacent to the pseudo-kinase domain (JH2). The function of the pseudo-kinase domain is to negatively regulate the activity of the kinase domain. An activating point mutation of JAK2 (JAK2-V617F, valine to phenylalanine substitution) in the pseudo-kinase domain has been identified in hematopoietic cells of patients with myeloproliferative disorders (MPD).[6] In particular, the JAK2-V617F mutation is found in >95% of patients with polycythemia vera (PV, characterized by overproduction of red blood cells), in ~50% of patients with essential thrombocythemia (ET, characterized by overproduction of platelets), and in ~50% of patients with myelofibrosis (MF, characterized by fibrosis of the bone marrow).[7] Moreover, disregulated JAK-STAT signaling has been identified in various inflammatory diseases and in a variety of cancers.[8] These findings together with several in vitro and in vivo data supported the hypothesis that inhibition of JAK2 presents an opportunity of targeted therapy for these myeloproliferative diseases.[9]

Accordingly, inhibitors with varying levels of JAK2 selectivity have been reported[10] and have entered clinical trials,[11] notably SAR302503,[12] lestaurtinib (CEP-701),[13] momelotinib (CYT387),[14] pacritinib,[15] gandotinib (LY2784544),[16] BMS-911543,[17] and

* Corresponding author. Tel.: +39 0331 581533; fax: +39 0331 581347.
E-mail address: gabriella.brasca@nervianoms.com (M.G. Brasca).

http://dx.doi.org/10.1016/j.bmc.2014.06.025
0968-0896/

AZD-1480.[18] Recently, ruxolitinib,[19] which displays equivalent activity against JAK1 and JAK2, with decreased activity against JAK3 and TYK2, has been approved by the FDA for the treatment of patients with MF, validating this target. However, the chronic dosing required for MPD treatment and the potential risk of immunosuppressive side effects related to inhibition of JAK1, JAK3, or TYK2 suggest to pursue the identification of a JAK2 selective inhibitor in order to increase safety.[20]

Due to high homology in the adenosine triphosphate (ATP) binding pocket among the JAK family kinases, the discovery of JAK2 inhibitors having JAK family selectivity has presented a significant challenge. Several interesting amino acid differences are found between the active sites of JAK kinases,[21] and indeed compounds with reasonable JAK family selectivity profile have been reported in recent years by different groups. However, it is not a trivial task to pin down the key elements underlying JAK family selectivity in order to rationally exploit them in the drug discovery process. Despite this difficulty, we initiated a program aimed at identifying potent inhibitors of JAK2 and possibly gaining a better insight into JAK family selectivity.

2. Chemistry

Compounds **2**–**34** were synthesized[22] according to Schemes 1–3. Preparation of amides **2**–**17**, and **25**–**34** was accomplished according to Scheme 1, starting from bromoketone **35**,[23] which was transformed into α-cyano-γ-ketoester **36**. Reaction of **36** with hydrobromic acid in acetic acid provided the 2-bromopyrrole **37**,[24] which was subjected to the Suzuki reaction in the presence of bis(triphenylphosphine) palladium(II) dichloride as catalyst with either commercially available or in-house synthesized[22a] aryl boronic acids, thus providing the corresponding 2-aryl pyrroles **38a**–**o**. Saponification of the carboxylic esters **38a**–**o** afforded **39a**–**o**, which were reacted with suitable amines under usual coupling condition to give **2**–**17**, and **25**–**34**. In Scheme 2, the preparation of compounds **18**–**19** and **23**–**24** is described. Alkylation of carboxylic ester **38e** with alkyl halides and cesium carbonate in *N*,*N*-dimethylformamide provided the corresponding derivatives **40a**–**b**. Final compounds **18**–**19** were obtained by hydrolysis of **40a**–**b** and subsequent amidation of carboxylic acid **41a**–**b** under usual coupling condition. Amino-pyrimidine **38e** and **40a** were converted into the corresponding iodo derivatives **42a**–**b** (Scheme 2). Palladium catalyzed coupling with 4-(4-methyl-piperazin-1-yl)-phenylamine furnished the arylamino derivatives **43a**–**b**. Hydrolysis of carboxylic esters **43a**–**b** gave the corresponding acids **44a**–**b**, which were submitted to the coupling reaction to provide amides **23**–**24**.

In Scheme 3, the preparation of pyrroles **20**–**22** is described using a completely different synthetic approach. Ketonitrile **46** was obtained by reacting commercially available methyl ester **45** with acetonitrile in the presence of potassium *tert*-pentoxide as base, in toluene at room temperature. Reaction of **46** with amino acetaldehyde diethylacetal followed by treatment with trifluoroacetic acid at room temperature afforded the pyrrole **47**. Its acetyl derivative **48** was reacted with *N*,*N*-dimethylformamide diisopropyl acetal and the enaminone was condensed with guanidine carbonate or formamidine acetate or methylguanidine hydrochloride to afford compounds **49**–**51**, respectively. Finally, conversion of nitriles **49**–**51** to amides **6**, **20**–**21** was performed under acidic condition. Alkylation of the amino group of **6** with 4–methoxybenzaldehyde under reductive amination condition furnished its benzylamino derivative **22**.

3. Results and discussion

Recently, we reported on a new chemical class of 5-heteroaryl-3-carboxamido-2-aryl pyrroles as Cdc7 inhibitors.[24] This work led to the identification of the potent Cdc7 inhibitor **1**, which also showed an encouraging activity against JAK2 (IC_{50} = 3.2 μM, Table 1). In the absence of the crystallographic data of Cdc7, a homology model based on the structure of CDK2 was used. The docking studies and the SAR of the 5-heteroaryl-3-carboxamido-2-aryl pyrroles correlate well with a modeled binding mode of **1** in the Cdc7 kinase homology model, where the nitrogen of the pyrimidinyl ring interacts with the hinge region, the amino group is directed towards the solvent, the carbonyl oxygen of the amide interacts with the conserved Lys and the aromatic group in position 2 of the pyrrole fits diagonally under the glycine-rich loop.

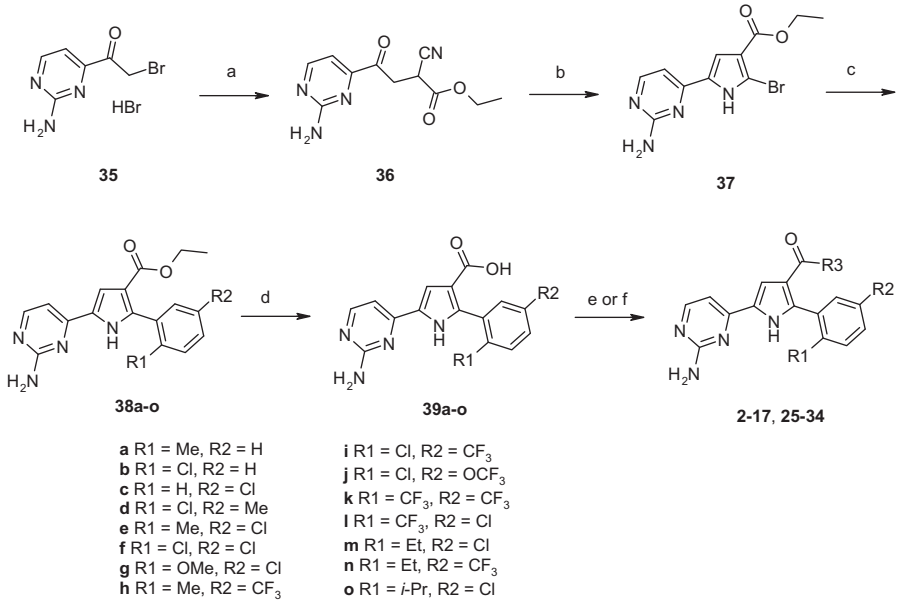

Scheme 1. Reagents and conditions: (a) ethyl cyanoacetate, NaOEt, DIPEA, THF, rt, overnight; (b) 33% HBr/AcOH, DCM, 0 °C to rt; (c) substituted boronic acid, LiCl, 1 M Na_2CO_3, $Pd(Ph_3P)_2Cl_2$, EtOH, toluene, 100 °C, 5 h; (d) 1.5 M KOH in 95% EtOH, reflux, 20 h; (e) HOBT·NH_3, EDCI, DIPEA, THF/DMF, rt, 3 h; (f) primary or secondary amines, EDCI, DIPEA, THF/DMF, rt, 3 h.

Please cite this article in press as: Brasca, M. G.; et al. *Bioorg. Med. Chem.* (2014), http://dx.doi.org/10.1016/j.bmc.2014.06.025

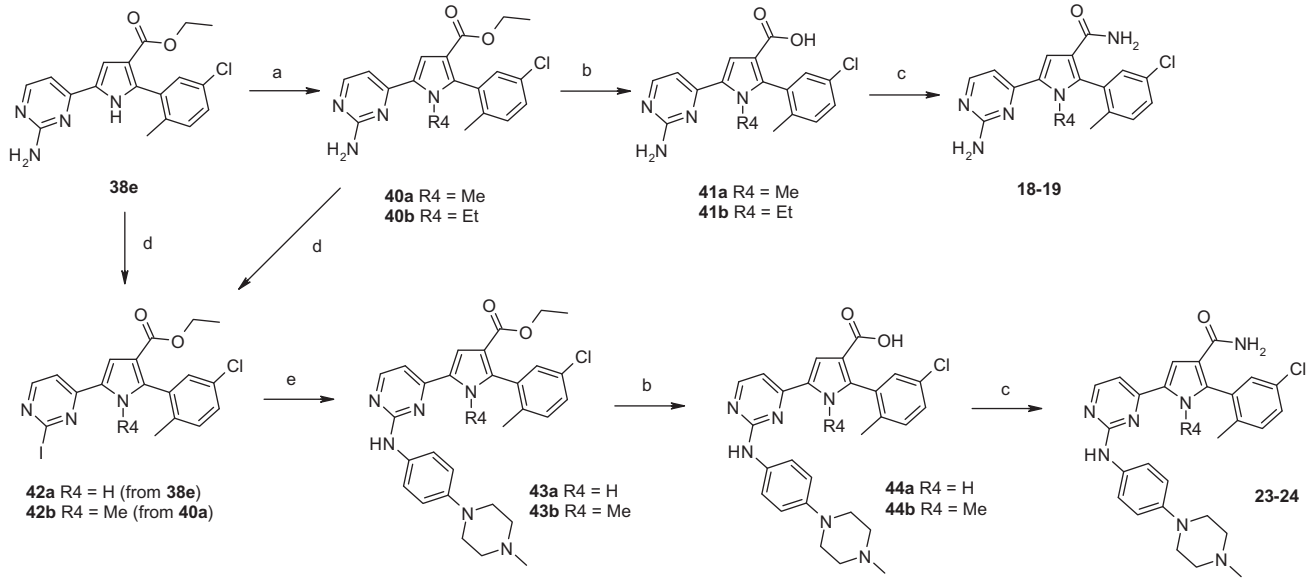

Scheme 2. Reagents and conditions: (a) R4X, Cs_2CO_3, DMF, rt, 3 h; (b) 2 N NaOH, EtOH, reflux, 3 h; (c) HOBT·NH_3, EDCI, DIPEA, THF/DMF, rt, 3 h; (d) CsI, CuI, I_2, *iso*-pentylnitrite, THF, reflux, 2 h; (e) $Pd(OAc)_2$, (±)-BINAP, K_2CO_3, DMF, 80 °C, 3 h.

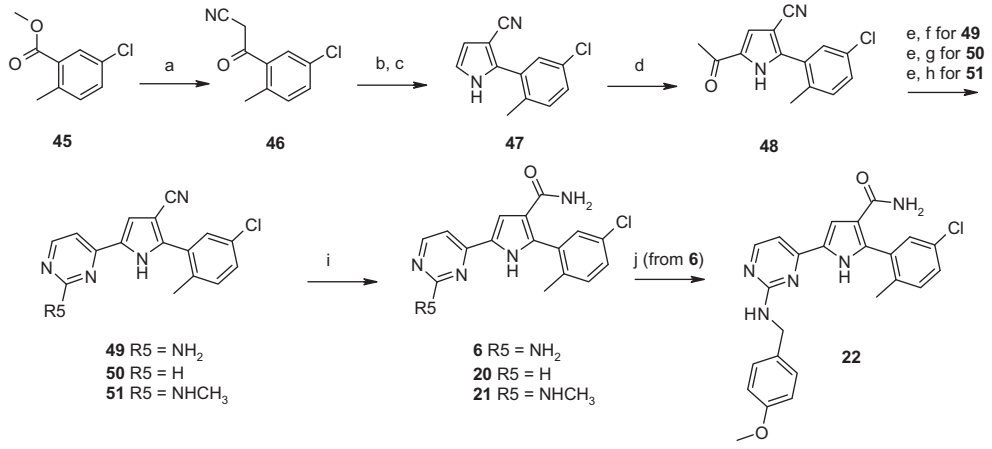

Scheme 3. Reagents and conditions: (a) acetonitrile, potassium *tert*-pentoxide 1.7 M in toluene, rt, 20 min; (b) amino acetaldehyde diethylacetal, toluene, reflux, 5 h; (c) TFA, rt, 30 min; (d) acetyl chloride, anhydrous aluminum trichloride, DCM, rt, 30 min; (e) *N*,*N*-dimethylformamide diisopropyl acetal, DMF, 90 °C, overnight; (f) guanidine carbonate, DMF, 5 h, 110 °C; (g) formamidine acetate, DMF, 5 h, 150 °C; (h) methylguanidine hydrochloride, K_2CO_3, DMF, 5 h, 110 °C; (i) TFA, H_2O, 98% H_2SO_4, 70 °C, 5 h; (j) 4-methoxybenzaldehyde, $NaBH(OAc)_3$, TFA, DMF, rt, overnight.

The screening of our corporate collection of compounds belonging to this class led to the identification of a small set of submicromolar inhibitors of JAK2 (**2**–**6**, Table 1). *Ortho* (**2**–**3**) and *meta* (**4**) substitution on the phenyl ring improved the affinity for JAK2 compared to **1**, while 2, 5 substitution pattern on the phenyl ring (**5**–**6**) appeared to be the best combination. In particular, compound **6** demonstrated high affinity for JAK2 and reduced potency against Cdc7 (IC_{50} = 0.360 μM).

To better understand the binding of these compounds, the crystal structure of **6** bound to the kinase domain of JAK2 was determined (Fig. 1A). Interestingly, the binding mode of compound **6** is significantly different from the model proposed for **1**, requiring a 180 degree rotation of the molecule. The nitrogen of the pyrimidine forms a hydrogen bond with the backbone NH of the hinge residue Leu932 and the amino group interacts with the backbone carbonyl of Glu930. Moreover, compound **6** is involved in a network of water mediated interactions with key residues in the active site: water molecule W1 mediates the interaction between the pyrrole nitrogen and water molecule W2, which, in turn, makes two hydrogen bonds to the backbone carbonyl of Gly993 and the side-chain of Asp994 (DFG motif). The carbonyl oxygen of the amide is directed towards the solvent and it interacts with the carboxylic residue of Asp939 via two other molecules of water (W3 and W4). W3 also establishes a hydrogen bond with the backbone NH of Ser936. The phenyl ring in position 2 is perpendicular to the pyrrole ring, adopting an orientation that allows it to direct the chlorine atom up towards the hydrophobic interior of the glycine-rich loop, while the methyl group is directed downwards into a shallow cavity defined by Arg980, Asn981, Leu983, Gly993, and Asp994 (Fig. 1B).

Based on the binding mode of compound **6**, we started an exploration of this class with the goal of generating compounds with potency against JAK2, selectivity for JAK2 over JAK1, JAK3, and TYK2, and in vivo efficacy with favourable pharmacokinetic and safety profile.

Our initial efforts were focused on analysis of R3, R4, and R5 substituents. Based on the structural analysis of the carboxamide moiety of **6**, exposed to the solvent area, a larger series of residues

Table 1
Preliminary exploration: R1, R2 substitution

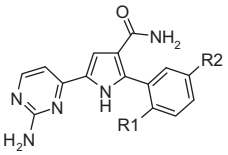

Compd	R1	R2	JAK2 IC_{50}, μM[a]
1	H	H	3.2
2	Me	H	0.695
3	Cl	H	0.615
4	H	Cl	0.617
5	Cl	Me	0.187
6	Me	Cl	0.020

[a] Values are means of three experiments.

linked to the pyrrole ring was investigated. Data concerning activity of analogues of **6** on JAK family enzymes are summarized in Table 2. Condensation of carboxylic acid **39e** with different amines gave rise to a series of amides **7**–**17**. The nature of the amide was essential to affinity, as deduced from the detrimental effect of a tertiary amide function on compound **8**. Small residues such as methyl (**7**) or linear alkyl bearing hydrophilic moieties (**10**–**11**) were tolerated, while ethyl residue (**9**) or straight alkyl bearing hydrophobic moieties (**12**–**13**) as well as bulkier and hydrophobic residues such as *iso*-butyl, benzyl and phenyl (**14**–**16**) caused a decrease of the inhibitory activity of JAK2. Instead, the presence of a bulky and hydrophilic moiety (**17**) was still tolerated. The biochemical selectivity of the most interesting compounds **6**, **7**, **11** and **17**, showing promising JAK2 potency (IC_{50} <50 nM, Table 2), was greater than six, five and threefold for JAK1, JAK3 and TYK2, respectively.

Introduction of methyl group as R4 substituent (**18**) showed a slight decrease in affinity for JAK2, when compared to **6**, probably due to the displacement of water molecule W1 and subsequent loss of the above described polar interactions between the pyrrole nitrogen of **6** and residues Gly993 and Asp994 (DFG) (Fig. 1A). More dramatic was the introduction of ethyl group (**19**), which caused a drop in affinity for JAK2.

From the SAR data in Table 2, it was clear that removal of the pyrimidinyl ring amino group (**20**) was deleterious due to the loss of interaction with the hinge region, while a small substituent on the amino group like a methyl (**21**) was tolerated. A benzyl moiety (**22**) led to a significant decrease in affinity. According to the observed binding mode of **6**, a further extension of the benzyl moiety into the active site is not likely to be tolerated due to a steric clash with the side-chain of the gatekeeper Met929. Interestingly, compounds **23** and **24**, bearing a bulky substituent as R5, showed appreciable affinity for JAK2.

In order to investigate this matter, the JAK2 structure with **24** was solved (Fig. 2), revealing the alternative binding mode of compound **1**, modelled into Cdc7. The aminopyrimidine moiety forms two hydrogen bonds with the backbone NH and the carbonyl of hinge residue Leu932. The carbonyl oxygen of the amide makes a direct hydrogen bond with the side-chain nitrogen of Lys882 and a water mediated interaction with the backbone NH of Asp994 (DFG), while the NH of the amide binds one of the side-chain oxygens of Asp994.

The superposition of the JAK2 structures with **6** and **24** shows the similarities and differences between the two inhibitor complexes (Fig. 3). In the hinge region, both inhibitors take advantage of the potential hydrogen bonds although they do so with different spatial orientation of the pyrimidine ring. Compound **6** directs the pyrimidine amino group towards the back of the pocket while **24** directs it towards the solvent. Both compounds interact with the

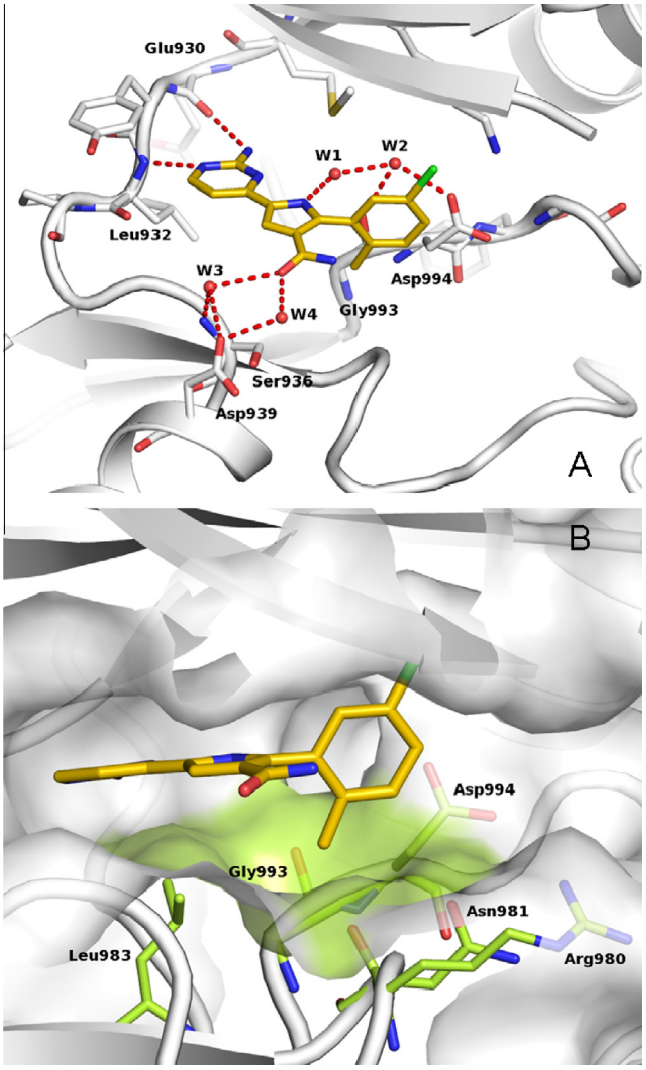

Figure 1. (A) Compound **6** bound to the active site of JAK2. Compound **6** is shown with yellow carbon atoms while protein is colored in white. Water molecules participating in the hydrogen bond network (W1, W2, W3, W4) are shown as red spheres and hydrogen bonds as red dashed lines. (B) Surface diagram showing how the aromatic group in position 2 is oriented perpendicular to the pyrrole ring, with the chlorine atom pointing up towards the glycine-rich loop and the methyl reaching down towards the cavity defined by Arg980, Asn981, Leu983, Gly993 and Asp994 (showed with green carbon atoms). The surface of the cavity is highlighted in green.

side-chain of Asp994, but **6** does so through two bridging water molecules, while **24** establishes a direct hydrogen bond between its amide nitrogen and the terminal oxygen of the DFG aspartate. The water molecules involved in the hydrogen bonding network for the two compounds are not equivalent. In particular, W2, found in the structure of JAK2 in complex with **6** and rather conserved in the published JAK2 structures, is not present in the structure of JAK2 in complex with **24**. Interestingly, both inhibitors place the 5-chloro-2-methylphenyl group underneath the glycine-rich loop although **6** manages to fit perfectly underneath the loop while **24** shifts the loop upwards, probably in order to avoid steric clashes with the substituted phenyl moiety. Finally, both inhibitors take advantage of the solvent exposed region although they do so from different points: **24** extends towards the solvent with the 4-(4-methylpiperazin-1-yl)phenyl moiety while **6** does so with its amide group.

Disappointingly, compounds **23** and **24** showed poor selectivity versus JAK3 and several other kinases of our panel (data not shown).

Table 2
Further exploration: R3, R4, R5 substitution

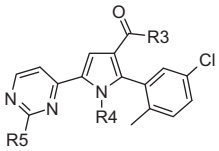

Compd	R3	R4	R5	JAK2 IC_{50}, μM[a]	JAK1/JAK2 selectivity[b]	JAK3/JAK2 selectivity[c]	TYK2/JAK2 selectivity[d]	SET-2 IC_{50}, μM[a,e]
6	NH_2	H	NH_2	0.020	13	6	4	0.43
7	NHMe	H	NH_2	0.035	10	9	8	0.48
8	$N(Me)_2$	H	NH_2	3.056	ND	ND	ND	ND
9	NHEt	H	NH_2	0.109	7	7	4	ND
10	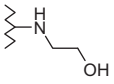	H	NH_2	0.057	13	7	7	ND
11	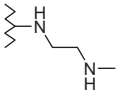	H	NH_2	0.044	7	8	6	>3.0
12		H	NH_2	0.114	4	5	5	ND
13	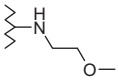	H	NH_2	0.268	7	6	6	ND
14		H	NH_2	0.384	2	10	3	ND
15	NHBz	H	NH_2	0.154	5	8	9	ND
16	NHPh	H	NH_2	0.247	0.5	14	2	ND
17	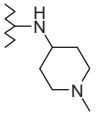	H	NH_2	0.046	>30	13	6	>3.0
18	NH_2	Me	NH_2	0.066	13	7	4	ND
19	NH_2	Et	NH_2	1.537	ND	ND	ND	ND
20	NH_2	H	H	1.235	ND	ND	ND	ND
21	NH_2	H	NHMe	0.043	6	3	4	1.01
22	NH_2	H	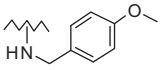	0.394	12	4	4	ND
23	NH_2	H	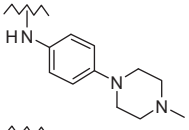	0.059	22	0.3	1	ND
24	NH_2	Me	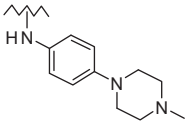	0.022	32	0.2	3	0.25

ND = not determined.
[a] Values are means of three experiments.
[b] JAK1 IC_{50}/JAK2 IC_{50}.
[c] JAK3 IC_{50}/JAK2 IC_{50}.
[d] TYK2 IC_{50}/JAK2 IC_{50}.
[e] Coefficient of variation (CV) <30%.

Compounds showing promising JAK2 potency (IC_{50} <50 nM, Table 2) were tested in JAK2 dependent human megakaryoblastic leukemic SET-2 cell line, derived from a patient with essential thrombocythemia and harboring the V617F mutation of JAK2.[25]

Interesting potency in the SET-2 cell proliferation assay was observed for compounds **6** and **7**, confirming activity as JAK2 inhibitors, whereas **11**, **17** and **21** showed lower antiproliferative activity, likely due to decreased cell permeability. In fact only moderate Caco2 permeability was observed for compounds **11** and **17** (data not shown), while compound **21** was not tested.

In order to characterize the selectivity within the JAK family of compounds **6** and **7** in cells, the IL-2 dependent T cell lymphoma DERL-7 cell line was used, since IL-2 induces JAK1 and JAK3, but not JAK2 activation in this line.[26] Moreover, the JAK independent

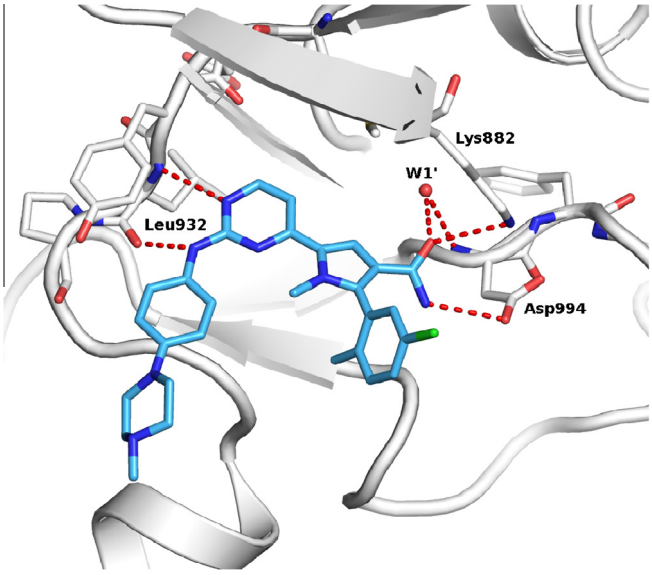

Figure 2. Compound **24** bound to the active site of JAK2. Compound **24** is shown with cyan carbon atoms while the protein is colored in white. Water molecule W1′ is shown as a red sphere and red dotted lines represent intermolecular hydrogen bonds.

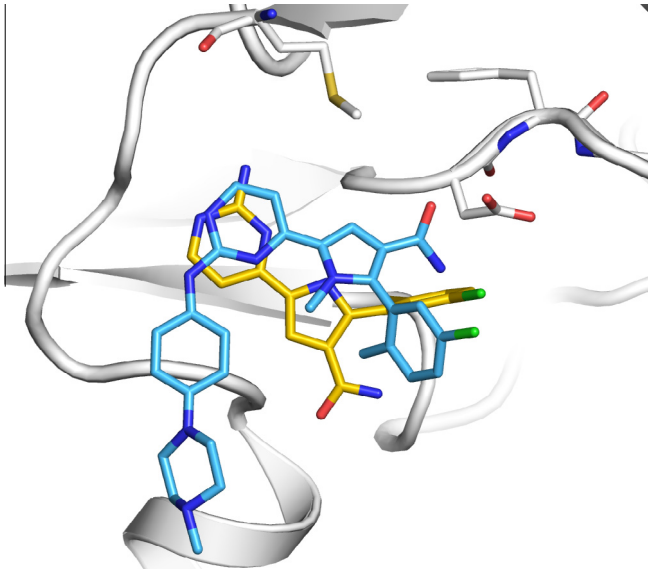

Figure 3. Overlay of the crystal structures of compounds **6** (yellow carbon atoms) and **24** (light blue carbon atoms) bound to JAK2 (shown in white) highlighting their remarkably different binding modes.

cell line A2780, which we have observed to be highly sensitive to antiproliferative agents, was used to assess general off target cytotoxicity (Table 3).

Compound **6** showed modest selectivity on DERL-7 cell line (less than twofold) and none in A2780 cell proliferation assay, while **7** seemed to be slightly more selective in these antiproliferative assays compared to **6**.

With the aim at improving the selectivity parameter both in biochemical assay and in cells, maintaining affinity for JAK2 and potency on SET-2 cell line, we decided to further investigate the 2, 5 substitution pattern on the phenyl ring (R1 and R2 groups).

It was observed that replacement of the substitution pattern of **6** (R1 = Me, R2 = Cl) was tolerated in several cases (Table 3). For example, **25** (R1, R2 = Cl), **27** (R1 = Me, R2 = CF_3) and **28** (R1 = Cl, R2 = CF_3) maintained good affinity for JAK2, while introduction of the methoxy group as R1 (**26**) caused a drastic reduction in binding affinity. The replacement of trifluomethyl of **28** with trifluomethoxy as R2 substituent (**29**) or substitution of chloro of **28** with trifluomethyl as R1 substituent (**30**) was still tolerated, but inversion of the substituents as in **31** (R1 = CF_3, R2 = Cl) caused a decrease in JAK2 affinity compared to **28**.

An improvement of biochemical selectivity for JAK2 over JAK1 was observed for **25**, **28**, and **30** compared to **6**, while only **25** showed enhanced selectivity for JAK2 over JAK3. Greater than fifteenfold biochemical selectivity for JAK2 over TYK2 was observed for **25** and **28**–**30**. Of particular interest was compound **28** since it exhibited a good potency in SET-2 antiproliferative assay and an improvement in the selectivity in DERL-7 and in A2780 cell proliferation assay (more than threefold).

The crystal structure of compound **28** bound to the kinase domain of JAK2 was solved (Fig. 4). The observed compound binding mode closely resembles that observed for compound **6**. The aminopyrimidine establishes the same two hydrogen bonds with the backbone of hinge residues Glu930 and Leu932 and the network of water mediated interactions described earlier is also conserved. The aromatic group is perpendicular to the pyrrole ring, and it directs the chlorine atom downwards into the cavity defined by Arg980, Asn981, Leu983, Gly993 and Asp994. The trifluoromethyl substituent, instead, points up towards the hydrophobic interior of the glycine-rich loop and forms two multipolar interactions with the carbonyl of Lys857 and Gly856.

Compound **28** shows better selectivity profile than compound **6** against JAK1 and TYK2 (Table 3). Most residues in close contact (monitored distance $\leqslant$5 Å) with the inhibitor are identical or highly similar in the three kinases. The main aminoacid differences are found in the solvent exposed region (JAK2 Asp939 → JAK1 Glu966), in the C-lobe side of the active site (JAK2 Ile982 → JAK1 Val1009, TYK2 Val1029) and in the glycine-rich loop (JAK2 Lys857 → JAK1 Glu883, TYK2 Glu905; JAK2 Asn859 → JAK1 His885, TYK2 His907; JAK2 Ser862 → JAK1 Lys888, TYK2 Lys910). Since compounds **6** and **28** differ in the kind of R1 and R2 substituents, we can hypothesize that the gain in selectivity against JAK1 and TYK2 derives from differences in the polarity and flexibility of the glycine-rich loop region that affect the van der Waals interactions network.

As said before, the crystal structure of **6** bound to the kinase domain of JAK2 shows that the methyl group (R1 substituent), linked to the aromatic ring, is directed downwards into a shallow cavity (Fig. 1B) formed by the Arg980, Asn981 Leu983, Gly993 and Asp994. While Gly993 is the residue immediately preceding the conserved DFG motif and is present in JAK2, JAK1, and TYK2, it is replaced by an alanine (Ala966) in JAK3.[21b,c] Targeting this area has proven useful in order to pursue selectivity towards JAK3,[16,18] where the presence of the bulkier and less flexible Ala966 instead of Gly993 reduces the size of the cavity and does not allow an optimal accommodation of the methyl group. To further explore this cavity, ethyl analogues of **6** and **27** were synthesized (**32** and **33**, respectively). Gratifyingly, insertion of ethyl group to the 2 position of the phenyl ring, which would extend deeper into this hydrophobic pocket, improved not only JAK2 biochemical activity but also cellular activity in SET-2 antiproliferative assay compared to the parent compounds **6** and **27**. Furthermore, **32** and **33** showed an improvement in the selectivity in DERL-7 (more than fourfold) and in A2780 cell proliferation assay (more than sixfold). A larger R1 substituent, such as *iso*-propyl (**34**), displayed fiftyfold weaker JAK2 affinity with respect to **32**, due to the shape and size of this pocket in JAK2.

In order to assess the potential of the most promising compounds **28**, **32**, and **33** further studies were performed. All compounds showed good solubility in neutral buffer and a preliminary pharmacokinetic study was evaluated in healthy nude

Table 3
Optimization: R1, R2, R3 substitution

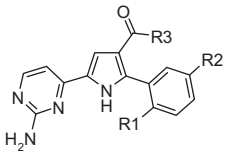

Compd	R1	R2	R3	JAK2 IC_{50}, μM[a]	JAK1/JAK2 selectivity[b]	JAK3/JAK2 selectivity[c]	TYK2/JAK2 selectivity[d]	SET-2 IC_{50}, μM[a,e]	DERL-7 IC_{50}, μM[a,e]	A2780 IC_{50}, μM[a,e]
6	Me	Cl	NH_2	0.020	13	6	4	0.43	0.74	0.38
7	Me	Cl	NHMe	0.035	10	9	8	0.48	2.07	0.98
25	Cl	Cl	NH_2	0.012	64	20	16	0.70	1.66	2.46
26	OMe	Cl	NH_2	0.308	32	11	ND	ND	ND	ND
27	Me	CF_3	NH_2	0.010	17	9	6	0.76	0.64	0.44
28	Cl	CF_3	NH_2	0.008	39	8	17	0.48	1.88	1.47
29	Cl	OCF_3	NH_2	0.024	18	4	18	1.10	ND	ND
30	CF_3	CF_3	NH_2	0.021	36	2	22	3.07	ND	ND
31	CF_3	Cl	NH_2	0.053	32	3	11	ND	ND	ND
32	Et	Cl	NH_2	0.003	8	11	3	0.21	0.88	2.00
33	Et	CF_3	NH_2	0.002	10	11	8	0.32	1.47	2.21
34	*iso*-Pr	Cl	NH_2	0.150	27	11	7	ND	ND	ND

ND = not determined.
[a] Values are means of three experiments.
[b] JAK1 IC_{50}/JAK2 IC_{50}.
[c] JAK3 IC_{50}/JAK2 IC_{50}.
[d] TYK2 IC_{50}/JAK2 IC_{50}.
[e] Coefficient of variation (CV) <30%.

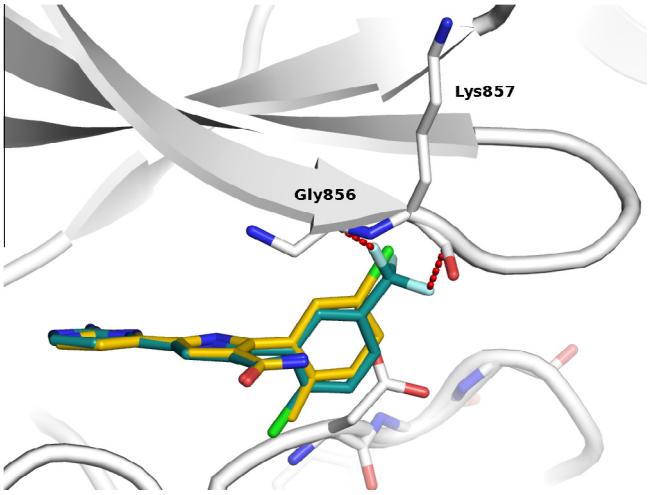

Figure 4. Overlay of **6** (yellow carbon atoms) and **28** (teal carbon atoms) bound to JAK2 (white ribbon). **28** maintains the same binding mode observed for **6**, but it is able to form two multipolar interactions with the backbone carbonyl of Gly856 and Lys857 of the glycine-rich loop.

mice (Table 4). When administered intravenously (iv) at 10 mg/kg, all compounds showed good exposure levels, as determined by the area under the curve (AUC), moderate clearance and a half life around 1 h, except for **32**, which showed high clearance and low AUC. Compound **28**, after oral administration at a dose of 10 mg/kg, showed the best pharmacokinetic parameters: interesting oral bioavailability (31%), with an AUC of 9.5 μM h and half life of 2.3 h.

Compound **28** displayed a combination of potency on JAK2, selectivity over related JAK family enzymes in biochemical and cellular assay, and physicochemical properties that made it suitable for further profiling as orally active JAK2 inhibitor. It was subsequently screened against an in-house panel of 52 serine-threonine and tyrosine kinases, showing more than twentyfold selectivity against all the unrelated kinases. Asides from internal profiling data, compound **28** was also tested in the KINOMEscan® screening platform that employs an active site directed competition binding assay to quantitatively measure interactions between test compound and 442 human kinases (including clinically relevant mutant kinases), covering >80% of the human catalytic protein kinome (KINOMEscan®, a division of DiscoveRx Corporation, San Diego, California, USA).[27] Results for primary screen binding interactions are reported as % Ctrl, where lower numbers indicate stronger hits in the matrix. At 0.1 μM, only JAK2, out of 442 kinases tested had % Ctrl <1. Outside the JAK family, only six kinases showed a binding between 1% and 10% Ctrl (CLK1, CLK2, CLK4, DYRK1A, DYRK1B, TAOK1). In agreement with that observed in our biochemical assays, the selectivity against the JAK family members was of five, twentyfour and one hundred and tenfold for JAK3, TYK2 and JAK1, respectively, (TREEspot™ image is included in the

Table 4
Solubility in neutral buffer and in vivo pharmacokinetic parameters in Balb nu/nu mice[a] of selected compounds

Compd	Solubility pH 7 (μM)	PK data (iv), 10 mg/kg[b]					PK data (po), 10 mg/kg[c]			
		C_{max} (μM)	AUC_{∞} (μM·h)	CL (mL/min/kg)	V_{ss} (L/kg)	$t_{1/2}$ (h)	C_{max} (μM)	AUC_{∞} (μM h)	$t_{1/2}$ (h)	*F* %
28	159	17.6	26.4	16.2	0.9	1.1	4.2	9.5	2.3	31
32	200	4.5	2.0	94.0	1.8	0.2	0.6	0.7	0.8	17
33	182	38.9	20.7	21.6	0.6	1.0	4.4	4.6	1.8	24

[a] *n* = 3 animals per study.
[b] Dosed in 10% Tween 80 in 5% dextrose.
[c] Dosed in 0.5% methocel.

Please cite this article in press as: Brasca, M. G.; et al. *Bioorg. Med. Chem.* (2014), http://dx.doi.org/10.1016/j.bmc.2014.06.025

Supporting information). All these data confirmed the high selectivity of **28**.

To further confirm the JAK2 selectivity of the compound **28** within the JAK family, we determined inhibition of the phosphorylation of constitutive STAT5 and STAT3 in the JAK2 dependent SET-2 cell line and inhibition of JAK1/3 induced STAT5 phosphorylation in IL-2 dependent DERL-7 cell line. In JAK2 dependent cell line (SET-2) compound **28** induced a dose-dependent reduction in the phosphorylated forms of STAT5 and STAT3 at doses consistent with inhibition of the proliferation ($\geqslant$0.2 μM), without affecting the total level of the respective proteins (Fig. 5). Instead, inhibition of JAK1/3 induced STAT5 phosphorylation in IL-2 dependent DERL-7 cell line was observed at higher doses ($\geqslant$2 μM), supporting the JAK2 selectivity also in cells.

The efficacy of **28** was evaluated in vivo in the SET-2 xenograft mouse model. As shown in Table 5 and Fig. 2 in Supporting information, **28** was orally administered at 15 and 30 mg/kg, twice a day, for 10 consecutive days in SCID mice. Both treatments resulted in significant tumour growth inhibition (TGI = 50% and 71%, respectively), associated with a moderate and reversible body weight loss (BWL = 6% at higher dose). A better efficacy profile for **28** was observed at higher dose (50 mg/kg, twice a day, 5 days on, 5 days off, for 3 cycles). This optimized schedule showed high efficacy (TGI = 95%), tumour regression and significant but reversible body weight loss (BWL = 15%).

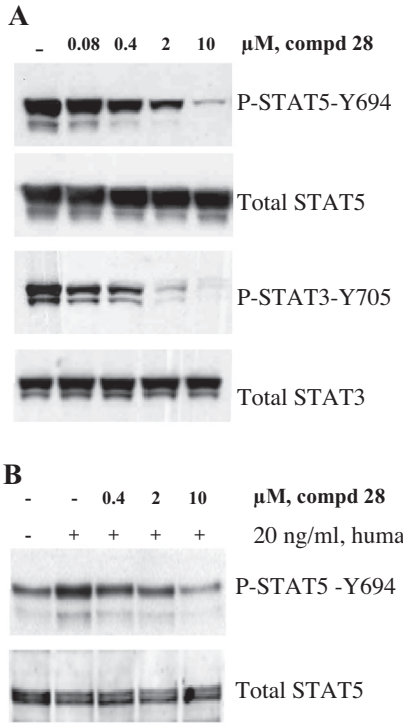

Figure 5. In vitro biomarkers modulation of compound **28**. (A) Inhibition of P-STAT5 and P-STAT3 in JAK2 dependent SET-2 cell line after 2 h of treatment with different concentrations of **28**. (B) Inhibition of P-STAT5 in DERL-7 cell line (JAK1/JAK3 dependent) activated by IL-2.

Table 5
In vivo activity of compound **28** in the SET-2 xenograft tumour model in SCID mice[a]

Treatment	Dose mg/kg	%TGI[b] (end of the treatment)	%BWL[c] (end of the treatment)
Bid 1-10 day	15	50	2
Bid 1-10 day	30	71	6
Bid 5 days on, 5 days off, for 3 cycles	50	95	15

[a] n = 7 animals per study.
[b] TGI = tumour growth inhibition.
[c] BWL = body weight loss.

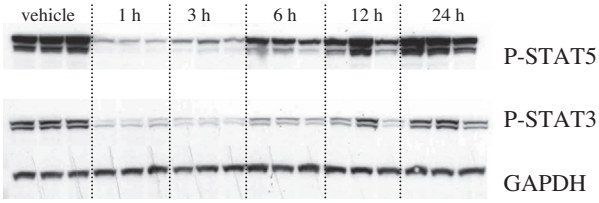

Figure 6. Ex-vivo biomarkers modulation in lysates from SET-2 xenograft model. Tumours (3 tumours/group) were isolated at different post-treatment times after single po administration of 50 mg/kg of compound **28**. Inhibition of P-STAT5 and P-STAT3 was analysed by Western Blot. Analysis of GAPDH was used as loading control.

After single administration of **28** in the SET-2 xenograft mouse model at 50 mg/kg, inhibition of the phosphorylation of STAT5 and STAT3 was observed up to 12 h post treatment, with maximal inhibition at 3 h (Fig. 6). At the dose of 30 mg/kg the tumours were analyzed at 1 and 3 h post treatment, and inhibition of phosphorylation of STAT proteins was confirmed (Fig. 3, Supporting information). These findings supported the mechanism of action of **28** as JAK2 inhibitor also in vivo and demonstrated the potent and durable in vivo activity of the compound.

4. Conclusion

The screening of our chemical collection led to the identification of compound **6**, displaying activity against JAK2. A structure based and medicinal chemistry driven optimization led to the identification of the potent and orally bioavailable JAK2 inhibitor **28** (NMS-P953), with selectivity over JAK family enzymes in biochemical and cellular assays. In vivo data in mice harboring SET-2 xenograft tumours demonstrated that the antitumour activity of compound **28** is related to the inhibition of JAK2, with a favourable pharmacokinetic and safety profile. NMS–P953 was selected for further characterization in additional tumour models that will be presented in due course.

5. Experimental

5.1. Chemistry

All solvents and reagents, unless otherwise stated, were commercially available, of the best grade and were used without further purification. All experiments dealing with moisture-sensitive compounds were carried out under dry nitrogen or argon atmosphere. Thin-layer chromatography was performed on Merck Silica Gel 60 F_{254} pre-coated plates. Column chromatography was conducted either under medium pressure on silica (Merck Silica Gel 40–63 μm) or performed by using a Biotage SP1 flash purification system with prepacked silica gel cartridges (Biotage or Varian). Components were visualized by UV light (λ: 254 nm) and by iodine vapor. ^{1}H NMR spectra were recorded at a constant temperature of 28 °C on a Varian INOVA 400 spectrometer (operating at 400.5 MHz for ^{1}H) and equipped with a 5 mm ^{1}H{^{13}C,^{15}N} z axis PFG indirect detection probe. Chemical shifts were referenced with respect to the residual solvents signals. Data are reported as follows: chemical shift (δ), multiplicity (s = singlet, d = doublet, t = triplet, q = quartet, br s = broad signal, td = triplet of doublet, dd = doublet of doublets, ddd = doublet of doublets of doublets, m = multiplet), coupling constants (Hz), and number of protons. HPLC–MS/UV analyses were performed on a LCQ DecaXP (Thermo, San Jose, US) ion trap instrument, equipped with an electrospray (ESI) ion source. The mass spectrometer is connected to a Surveyor

HPLC system (Thermo, San Jose, US) with an UV photodiode array detector (UV detection 215–400 nm). A Phenomenex Gemini C18 110 Å, LC column 50 × 4.6 mm, 3 μm particle size was used. Mobile phase A was ammonium acetate 5 mM buffer (pH 4.5 with acetic acid)/acetonitrile 95:5, and mobile phase B was ammonium acetate 5 mM buffer (pH 4.5 with acetic acid)/acetonitrile 5:95. Gradient from 0% to 100% B in 7 min, hold 100% B 2 min. Flow rate 1 mL/min. Injection volume 10 μL. Full scan, mass range from 50 to 1200 amu. Heated capillary temperature was 275 °C and spray voltage value was set at 4 kV. Mass are given as *m*/*z* ratio. Instrument control, data acquisition and processing were performed by using Xcalibur 2.1 software (Thermo). As formerly reported,[28] ESI(+) high–resolution mass spectra (HRMS) were obtained on a Q-Tof Ultima (Waters, Manchester, UK) mass spectrometer directly connected with a Agilent 1100 micro–HPLC system (Palo Alto, CA, US). GC–MS analyses were performed on a GCQ (FinniganMAT) ion trap instrument, equipped with an electron (EI) ion source. The mass spectrometer is connected to a Trace CG system (Thermo, San Jose, US) through a transfer line. A DB-5MS (J&W Scientific), 30 m × 0.25 mm I.D., film 0.25 μm was used. Temperature gradient from 60 °C (hold 1 min) to 280 °C (hold 10 min) in 12 min. Injector temperature was 280 °C and the transfer line temperature was 250 °C. Full scan, mass range from 35 to 650 amu. Source temperature was 200 °C. Electron energy was 70 eV.

5.1.1. 5-(2-Aminopyrimidin-4-yl)-2-phenyl-1*H*-pyrrole-3-carboxamide (1)

From ethyl 3-oxo-3-phenyl-propionate and 1-(2-aminopyrimidin-4-yl)-2-bromoethanone hydrobromide (**35**) according to a described procedure.[24]

5.1.2. 5-(2-Aminopyrimidin-4-yl)-2-(5-chloro-2-methylphenyl)-1*H*-pyrrole-3-carboxamide (6)

Ethyl cyanoacetate (5.3 mL, 50 mmol) was added to a suspension of sodium (1.15 g, 50 mmol) in 150 mL of anhydrous EtOH at 0 °C. After 20 min at room temperature, the reaction mixture was concentrated and the resultant solid was added to a solution of 1-(2-aminopyrimidin-4-yl)-2-bromoethanone hydrobromide (**35**, 14.85 g, 50 mmol) and *N*,*N*-diisopropylethylamine (8.8 mL, 50 mmol) in anhydrous THF (300 mL). The reaction mixture was stirred overnight at room temperature, concentrated and the residue was suspended in water and extracted with DCM. The organic extracts were dried over sodium sulfate and concentrated. The crude was purified by flash chromatography (DCM/MeOH 95:5) to give ethyl 4-(2-aminopyrimidin-4-yl)-2-cyano-4-oxobutanoate (**36**, 5.16 g, 41%). ^{1}H NMR (400 MHz, DMSO-d_6) δ 8.52 (d, J = 4.9 Hz, 1H), 6.97 (d, J = 4.9 Hz, 1H), 4.56 (t, J = 5.6 Hz, 1H), 4.19 (q, J = 7.1 Hz, 2H), 3.74 (d, J = 5.6 Hz, 2H), 1.21 (t, J = 7.1 Hz, 3H); LC–MS (ESI): *m*/*z* 249 $[M+H]^+$; HRMS (ESI): *m*/*z* calcd for $C_{11}H_{12}N_4O_3$+H^+ 249.0982, found 249.0975.

A suspension of **36** (5.0 g, 20.14 mmol) in DCM (40 mL) was added dropwise to 33% HBr in AcOH (40 mL) at 0 °C. The mixture was left at 0 °C for 30 min and then at room temperature until disappearance of the starting material. The solid was filtered, washed with DCM, neutralized with 7 N NH_3 in MeOH to afford ethyl 5-(2-aminopyrimidin-4-yl)-2-bromo-1*H*-pyrrole-3-carboxylate (**37**, 5.5 g, 88%). ^{1}H NMR (400 MHz, DMSO-d_6) δ 12.84 (br s, 1H), 8.22 (d, J = 5.4 Hz, 1H), 7.23 (s, 1H), 6.99 (d, J = 5.1 Hz, 1H), 6.42 (br s, 2H), 4.21 (q, J = 7.1 Hz, 2H), 1.29 (t, J = 7.1 Hz, 3H); LC–MS (ESI): *m*/*z* 312 $[M+H]^+$; HRMS (ESI): *m*/*z* calcd for $C_{11}H_{11}BrN_4O_2$+H^+ 311.0138, found 311.0139.

To a solution of **37** (2.0 g, 6.43 mmol) dissolved in EtOH (20 mL) and toluene (20 mL), LiCl (408 mg, 9.64 mmol), 1 M aq Na_2CO_3 (17 mmol), 5-chloro-2-methylphenylboronic acid (1.423 g, 8.35 mmol) were added. The resulting reaction mixture was degassed three times back filling with argon each time before being charged with $Pd(Ph_3P)_2Cl_2$ (470 mg, 0.67 mmol), degassed four times back filling with argon each time and then heated at 100 °C for 5 h. After cooling to room temperature, the precipitate was filtered and the filtrate was evaporated under reduced pressure, dissolved in DCM and washed with water. The organic layer was then dried over sodium sulfate and concentrated. The crude material was chromatographed on silica gel (DCM/EtOAc 50:50) to afford ethyl 5-(2-aminopyrimidin-4-yl)-2-(5-chloro-2-methylphenyl)-1*H*-pyrrole-3-carboxylate (**38e**, 1.99 g, 87%). ^{1}H NMR (400 MHz, DMSO-d_6) δ 12.18 (br s, 1H), 8.21 (d, J = 5.2 Hz, 1H), 7.40 (dd, J = 8.2, 2.2 Hz, 1H), 7.27–7.34 (m, 3H), 7.01 (d, J = 5.2 Hz, 1H), 6.41 (s, 2H), 4.04 (q, J = 7.1 Hz, 2H), 2.11 (s, 3H), 1.09 (t, J = 7.1 Hz, 3H); LC–MS (ESI): *m*/*z* 357 $[M+H]^+$; HRMS (ESI): *m*/*z* calcd for $C_{18}H_{17}ClN_4O_2$+H^+ 357.1113, found 357.1115.

The intermediate **38e** (1.0 g, 2.80 mmol) was treated with 1.5 M KOH in 95% EtOH (37.3 mL, 20 equiv) under reflux for 20 h. After cooling, the residue was concentrated, dissolved in water and washed with DCM. A solution of 2 N HCl was added, under agitation, to the aqueous phase cooled to 5 °C. The resultant precipitate was collected by filtration to give 5-(2-aminopyrimidin-4-yl)-2-(5-chloro-2-methylphenyl)-1*H*-pyrrole-3-carboxylic acid (**39e**, 0.92 g, 95%). ^{1}H NMR (400 MHz, DMSO-d_6) δ 12.54 (br s, 1H), 12.06 (s, 1H), 8.28 (d, J = 6.5 Hz, 1H), 7.77 (br s, 1H), 7.59 (d, J = 2.6 Hz, 1H), 7.40–7.45 (m, 1H), 7.28–7.37 (m, 3H), 2.12 (s, 3H); LC–MS (ESI): *m*/*z* 329 $[M+H]^+$; HRMS (ESI): *m*/*z* calcd for $C_{16}H_{13}ClN_4O_2$+H^+ 329.0800, found 329.0799.

A solution of **39e** (470 mg, 1.43 mmol) in DMF/THF (1/1, 5 mL) and *N*,*N*-diisopropylethylamine (1.02 mL, 5.86 mmol) was stirred at 0 °C. EDCI (594 mg, 3.1 mmol) and HOBT·NH_3 (430 mg, 2.79 mmol) were added and the reaction mixture was stirred for 3 h at room temperature. The mixture was dropped into a saturated solution of $NaHCO_3$ and ice and the resulting precipitate was collected by filtration to afford **6** (384 mg, 82%). ^{1}H NMR (400 MHz, DMSO-d_6) δ 11.84 (br s, 1H), 8.19 (d, J = 5.2 Hz, 1H), 7.32–7.40 (m, 2H), 7.26–7.30 (m, 2H), 7.22 (br s, 1H), 6.93 (d, J = 5.2 Hz, 1H), 6.73 (br s, 1H), 6.32 (br s, 2H), 2.12 (s, 3H); LC–MS (ESI): *m*/*z* 328 $[M+H]^+$; HRMS (ESI): *m*/*z* calcd for $C_{16}H_{14}ClN_5O$+H^+ 328.0960, found 328.0959.

The following compounds **2**–**5**, and **25**–**34** were prepared according to the method described above using the suitable aryl boronic acid.

5.1.3. 5-(2-Aminopyrimidin-4-yl)-2-(2-methylphenyl)-1*H*-pyrrole-3-carboxamide (2)

^{1}H NMR (400 MHz, DMSO-d_6) δ 12.29 (br s, 1H), 8.24 (d, J = 6.5 Hz, 1H), 7.74 (br s, 2H), 7.62 (d, J = 2.1 Hz, 1H), 7.24–7.39 (m, 3H), 7.22 (d, J = 6.5 Hz, 1H), 7.04 (br s, 1H), 6.87 (br s, 1H), 2.16 (s, 3H); LC–MS (ESI): *m*/*z* 294 $[M+H]^+$; HRMS (ESI): *m*/*z* calcd for $C_{16}H_{15}N_5O$+H^+ 294.1350, found 294.1350.

5.1.4. 5-(2-Aminopyrimidin-4-yl)-2-(2-chlorophenyl)-1*H*-pyrrole-3-carboxamide (3)

^{1}H NMR (400 MHz, DMSO-d_6) δ 11.89 (br s, 1H), 8.19 (d, J = 5.2 Hz, 1H), 7.49–7.54 (m, 1H), 7.35–7.46 (m, 3 H), 7.33 (d, J = 2.6 Hz, 1H), 7.19 (br s, 1H), 6.93 (d, J = 5.2 Hz, 1H), 6.69 (br s, 1H), 6.33 (br s, 2H); LC–MS (ESI): *m*/*z* 314 $[M+H]^+$; HRMS (ESI): *m*/*z* calcd for $C_{15}H_{12}ClN_5O$+H^+ 314.0803, found 314.0804.

5.1.5. 5-(2-Aminopyrimidin-4-yl)-2-(3-chlorophenyl)-1*H*-pyrrole-3-carboxamide (4)

^{1}H NMR (400 MHz, DMSO-d_6) δ 11.79 (br s, 1H), 8.22 (d, J = 5.2 Hz, 1H), 7.73 (t, J = 1.8 Hz, 1H), 7.62 (td, J = 1.7, 7.1 Hz, 1H), 7.48 (br s, 1H), 7.46 (br s, 1H), 7.42 (t, J = 7.9 Hz, 1H), 7.28 (d, J = 2.4 Hz, 1H), 7.01 (d, J = 5.2 Hz, 1H), 6.90 (br s, 1H), 6.38 (br s, 2H); LC–MS (ESI): *m*/*z* 314 $[M+H]^+$; HRMS (ESI): *m*/*z* calcd for $C_{15}H_{12}ClN_5O$+H^+ 314.0803, found 314.0807.

5.1.6. 5-(2-Aminopyrimidin-4-yl)-2-(2-chloro-5-methylphenyl)-1*H*-pyrrole-3-carboxamide (5)

^{1}H NMR (400 MHz, DMSO-d_6) δ 11.85 (br s, 1H), 8.19 (d, J = 5.2 Hz, 1H), 7.38 (d, J = 8.2 Hz, 1H), 7.31 (d, J = 2.6 Hz, 1H), 7.25 (m, 1H), 7.20–7.24 (m, 1H), 7.14 (br s, 1H), 6.93 (d, J = 5.2 Hz, 1H), 6.68 (br s, 1H), 6.33 (br s, 2H), 2.32 (s, 3H); LC–MS (ESI): m/z 328 $[M+H]^+$; HRMS (ESI): m/z calcd for $C_{16}H_{14}ClN_5O+H^+$ 328.0960, found 328.0965.

5.1.7. 5-(2-Aminopyrimidin-4-yl)-2-(2,5-dichlorophenyl)-1*H*-pyrrole-3-carboxamide (25)

^{1}H NMR (400 MHz, DMSO-d_6) δ 12.35 (br s, 1H), 8.26 (d, J = 6.1 Hz, 1H), 7.43–7.58 (m, 7H), 7.09 (d, J = 6.1 Hz, 1H), 6.87 (br s, 1H); LC–MS (ESI): m/z 348 $[M+H]^+$; HRMS (ESI): m/z calcd for $C_{15}H_{11}Cl_2N_5O+H^+$ 348.0414, found 348.0419.

5.1.8. 5-(2-Aminopyrimidin-4-yl)-2-(5-chloro-2-methoxyphenyl)-1*H*-pyrrole-3-carboxamide (26)

^{1}H NMR (400 MHz, DMSO-d_6) δ 11.63 (br s, 1H), 8.19 (d, J = 5.2 Hz, 1H), 7.36–7.41 (m, 2H), 7.25 (d, J = 2.6 Hz, 1H), 7.20 (br s, 1H), 7.08–7.12 (m, 1H), 6.92 (d, J = 5.2 Hz, 1H), 6.74 (br s, 1H), 6.35 (s, 2H), 3.75 (s, 3H); LC–MS (ESI): m/z 344 $[M+H]^+$; HRMS (ESI): m/z calcd for $C_{16}H_{14}ClN_5O_2+H^+$ 344.0909, found 344.0915.

5.1.9. 5-(2-Aminopyrimidin-4-yl)-2-[2-methyl-5-(trifluoromethyl) phenyl]-1*H*-pyrrole-3-carboxamide (27)

^{1}H NMR (400 MHz, DMSO-d_6) δ 11.91 (br s, 1H), 8.20 (d, J = 5.2 Hz, 1H), 7.64 (dd, J = 1.5, 8.1 Hz, 1H), 7.53 (d, J = 1.5 Hz, 1H), 7.49 (d, J = 8.1 Hz, 1H), 7.37 (d, J = 2.4 Hz, 1H), 7.32 (br s, 1H), 6.92 (d, J = 5.2 Hz, 1H), 6.74 (br s, 1H), 6.32 (br s, 2H), 2.23 (s, 3H); LC–MS (ESI): m/z 362 $[M+H]^+$; HRMS (ESI): m/z calcd for $C_{17}H_{14}F_3N_5O+H^+$ 362.1223, found 362.1225.

5.1.10. 5-(2-Aminopyrimidin-4-yl)-2-[2-chloro-5-(trifluoromethyl) phenyl]-1*H*-pyrrole-3-carboxamide (28)

^{1}H NMR (400 MHz, DMSO-d_6) δ 12.07 (br s, 1H), 8.22 (d, J = 5.3 Hz, 1H), 7.71–7.81 (m, 3H), 7.40–7.44 (m, 1H), 7.37 (d, J = 2.4 Hz, 1H), 6.90 (d, J = 5.3 Hz, 1H), 6.76 (br s, 1H), 6.35 (br s, 2H); LC–MS (ESI): m/z 382 $[M+H]^+$; HRMS (ESI): m/z calcd for $C_{16}H_{11}ClF_3N_5O+H^+$ 382.0677, found 382.0677.

5.1.11. 5-(2-Aminopyrimidin-4-yl)-2-[2-chloro-5-(trifluoro-methoxy)phenyl]-1*H*-pyrrole-3-carboxamide (29)

^{1}H NMR (400 MHz, DMSO-d_6) δ 12.04 (br s, 1H), 8.21 (d, J = 5.2 Hz, 1H), 7.64 (ddd, J = 1.1, 1.5, 8.8 Hz, 1H), 7.41–7.46 (m, 2H), 7.39 (br s, 1H), 7.30 (d, J = 2.4 Hz, 2H), 6.90 (d, J = 5.1 Hz, 1H), 6.76 (br s, 1H), 6.35 (b s, 2H); LC–MS (ESI): m/z 398 $[M+H]^+$; HRMS (ESI): m/z calcd for $C_{16}H_{11}ClF_3N_5O_2+H^+$ 398.0626, found 398.0624.

5.1.12. 5-(2-Aminopyrimidin-4-yl)-2-[2,5-bis(trifluoromethyl) phenyl]-1*H*-pyrrole-3-carboxamide (30)

^{1}H NMR (400 MHz, DMSO-d_6) δ 12.08 (br s, 1H), 8.21 (d, J = 5.2 Hz, 1H), 7.79 (br s, 1H), 7.37 (d, J = 2.4 Hz, 1H), 6.85 (d, J = 5.2 Hz, 1H), 6.34 (br s, 2H); LC–MS (ESI): m/z 416 $[M+H]^+$; HRMS (ESI): m/z calcd for $C_{17}H_{11}F_6N_5O+H^+$ 416.0941, found 416.0945.

5.1.13. 5-(2-Aminopyrimidin-4-yl)-2-[5-chloro-2-(trifluoro-methyl)phenyl]-1*H*-pyrrole-3-carboxamide (31)

^{1}H NMR (400 MHz, DMSO-d_6) δ 12.03 (br s, 1H), 8.21 (d, J = 5.4 Hz, 1H), 7.95 (s, 1H), 7.80 (d, J = 8.5 Hz, 1H), 7.70 (dd, J = 1.4, 8.5 Hz, 1H), 7.54 (d, J = 1.9 Hz, 1H), 7.35 (d, J = 2.6 Hz, 1H), 7.34 (br s, 1H), 6.86 (d, J = 5.2 Hz, 1H), 6.68 (br s, 1H), 6.36 (br s, 2H); LC–MS (ESI): m/z 382 $[M+H]^+$; HRMS (ESI): m/z calcd for $C_{16}H_{11}ClF_3N_5O+H^+$ 382.0677, found 382.0679.

5.1.14. 5-(2-Aminopyrimidin-4-yl)-2-(5-chloro-2-ethylphenyl)-1*H*-pyrrole-3-carboxamide (32)

^{1}H NMR (400 MHz, DMSO-d_6) δ 11.87 (br s, 1H), 8.19 (d, J = 5.4 Hz, 1H), 7.40 (dd, J = 2.3, 8.3 Hz, 1H), 7.34 (d, J = 2.7 Hz, 1H), 7.32 (d, J = 8.3 Hz, 1H), 7.25 (d, J = 2.2 Hz, 1H), 7.16 (br s, 1H), 6.92 (d, J = 5.2 Hz, 1H), 6.71 (br s, 1H), 6.32 (br s, 2H), 2.46 (q, J = 7.6 Hz, 2H), 0.97 (t, J = 7.6 Hz, 3H); LC–MS (ESI): m/z 342 $[M+H]^+$; HRMS (ESI): m/z calcd for $C_{17}H_{16}ClN_5O+H^+$ 342.1116, found 342.1116.

5.1.15. 5-(2-Aminopyrimidin-4-yl)-2-[2-ethyl-5-(trifluoromethyl) phenyl]-1*H*-pyrrole-3-carboxamide (33)

^{1}H NMR (400 MHz, DMSO-d_6) δ 11.93 (br s, 1H), 8.19 (d, J = 5.2 Hz, 1H), 7.69 (dd, J = 1.5, 8.1 Hz, 1H), 7.53 (d, J = 8.1 Hz, 1H), 7.50 (d, J = 1.6 Hz, 1H), 7.37 (d, J = 2.6 Hz, 1H), 7.27 (br s, 1H), 6.91 (d, J = 5.2 Hz, 1H), 6.71 (br s, 1H), 6.32 (br s, 2H), 2.56 (q, J = 7.5 Hz, 2H), 1.01 (t, J = 7.6 Hz, 3H); LC–MS (ESI): m/z 376 $[M+H]^+$; HRMS (ESI): m/z calcd for $C_{18}H_{16}F_3N_5O+H^+$ 376.1380, found 376.1382.

5.1.16. 5-(2-Aminopyrimidin-4-yl)-2-[5-chloro-2-(propan-2-yl) phenyl]-1*H*-pyrrole-3-carboxamide (34)

^{1}H NMR (400 MHz, DMSO-d_6) δ 11.89 (br s, 1H), 8.18 (d, J = 5.2 Hz, 1H), 7.44 (dd, J = 2.3, 8.3 Hz, 1H), 7.38 (d, J = 8.3 Hz, 1H), 7.34 (d, J = 2.7 Hz, 1H), 7.21 (d, J = 2.3 Hz, 1H), 7.11 (br s, 1H), 6.91 (d, J = 5.2 Hz, 1H), 6.71 (br s, 1H), 6.32 (br s, 2H), 2.79 (spt, J = 6.9 Hz, 1H), 1.06 (d, J = 6.8 Hz, 6H); LC–MS (ESI): m/z 356 $[M+H]^+$; HRMS (ESI): m/z calcd for $C_{18}H_{18}ClN_5O+H^+$ 356.1273, found 356.1271.

5.1.17. 5-(2-Aminopyrimidin-4-yl)-2-(5-chloro-2-methylphenyl)-*N*-methyl-1*H*-pyrrole-3-carboxamide (7)

To a solution of **39e** (142 mg, 0.43 mmol) in DMF/THF (1:1, 3 mL) DIPEA (0.301 mL, 1.72 mmol) and $MeNH_2$ 2 M solution in THF (0.432 mL, 0.86 mmol) were added and the solution was stirred at 0 °C. EDCI (157 mg, 0.86 mmol) and HOBT (117 mg, 0.86 mmol) were added and the reaction mixture was stirred for 3 h at room temperature. The mixture was diluted with water and extracted with DCM (4 × 10 mL). The organic phase was washed with brine, water and then dried over sodium sulfate and concentrated. The crude material was chromatographed on silica gel (DCM/MeOH 90:10) to afford **7** (124 mg, 84%).

^{1}H NMR (400 MHz, DMSO-d_6) δ 11.84 (br s, 1H), 8.19 (d, J = 5.4 Hz, 1H), 7.80 (q, J = 4.8 Hz, 1H), 7.35 (dd, J = 2.3, 8.3 Hz, 1H), 7.31 (d, J = 2.6 Hz, 1H), 7.27 (d, J = 2.3 Hz, 1H), 7.28 (d, J = 8.0 Hz, 1H), 6.93 (d, J = 5.2 Hz, 1H), 6.32 (br s, 1H), 2.62 (d, J = 4.5 Hz, 3H), 2.10 (s, 3H); LC–MS (ESI): m/z 342 $[M+H]^+$; HRMS (ESI): m/z calcd for $C_{17}H_{16}ClN_5O+H^+$ 342.1116, found 342.1118.

The following compounds **8**–**17** were prepared according to the method described above using the suitable amine.

5.1.18. 5-(2-Aminopyrimidin-4-yl)-2-(5-chloro-2-methylphenyl)-*N*,*N*-dimethyl-1*H*-pyrrole-3-carboxamide (8)

^{1}H NMR (400 MHz, DMSO-d_6) δ 11.84 (br s, 1H), 8.19 (d, J = 5.2 Hz, 1H), 7.35 (dd, J = 2.3, 8.3 Hz, 1H), 7.29 (d, J = 2.2 Hz, 1H), 7.30 (d, J = 8.1 Hz, 1H), 7.00 (s, 1H), 6.99 (d, J = 5.2 Hz, 1H), 6.36 (s, 1H), 2.84 (s, 6H), 2.17 (s, 3H); LC–MS (ESI): m/z 356 $[M+H]^+$; HRMS (ESI): m/z calcd for $C_{18}H_{18}ClN_5O+H^+$ 356.1273, found 356.1278.

5.1.19. 5-(2-Aminopyrimidin-4-yl)-2-(5-chloro-2-methylphenyl)-*N*-ethyl-1*H*-pyrrole-3-carboxamide (9)

^{1}H NMR (400 MHz, DMSO-d_6) δ 11.83 (br s, 1H), 8.19 (d, J = 5.2 Hz, 1H), 7.80 (t, J = 5.7 Hz, 1H), 7.35 (dd, J = 2.3, 8.3 Hz, 1H), 7.33 (d, J = 2.6 Hz, 1H), 7.28 (d, J = 8.3 Hz, 1H), 7.28 (d, J = 2.3 Hz, 1H), 6.94 (d, J = 5.2 Hz, 1H), 6.32 (br s, 2H), 3.12 (dq,

J = 5.7, 7.2 Hz, 2H), 2.11 (s, 3H), 1.02 (t, J = 7.2 Hz, 3H); LC–MS (ESI): m/z 356 $[M+H]^+$; HRMS (ESI): m/z calcd for $C_{18}H_{18}ClN_5O+H^+$ 356.1273, found 356.1277.

5.1.20. 5-(2-Aminopyrimidin-4-yl)-2-(5-chloro-2-methylphenyl)-*N*-(2-hydroxyethyl)-1*H*-pyrrole-3-carboxamide (10)

^{1}H NMR (400 MHz, DMSO-d_6) δ 11.86 (br s, 1H), 8.20 (d, J = 5.4 Hz, 1H), 7.71 (t, J = 5.8 Hz, 1H), 7.32–7.38 (m, 2H), 7.23–7.30 (m, 2H), 6.94 (d, J = 5.2 Hz, 1H), 6.34 (br s, 2H), 4.61 (t, J = 5.4 Hz, 1H), 3.38–3.44 (m, 2H), 3.17 (q, J = 6.1 Hz, 2H), 2.10 (s, 3H); LC–MS (ESI): m/z 372 $[M+H]^+$; HRMS (ESI): m/z calcd for $C_{18}H_{18}ClN_5O_2+H^+$ 372.1222, found 372.1230.

5.1.21. 5-(2-Aminopyrimidin-4-yl)-2-(5-chloro-2-methylphenyl)-*N*-[2-(methylamino)ethyl]-1*H*-pyrrole-3-carboxamide (11)

Compound **11** was obtained from *tert*-butyl [2-({[5-(2-aminopyrimidin-4-yl)-2-(5-chloro-2-methylphenyl)-1*H*-pyrrol-3-yl]carbonyl}amino)ethyl]methylcarbamate (prepared according to the method described above) after treatment with 50% CF_3COOH in DCM.

^{1}H NMR (400 MHz, DMSO-d_6) δ 11.86 (br s, 1H), 8.19 (d, J = 5.2 Hz, 1H), 7.66 (t, J = 5.7 Hz, 1H), 7.36 (dd, J = 2.2, 8.2 Hz, 1H), 7.33 (s, 1H), 7.29 (d, J = 2.3 Hz, 1H), 7.29 (d, J = 8.2 Hz, 1H), 6.94 (d, J = 5.2 Hz, 1H), 6.33 (br s, 2H), 3.18 (q, J = 6.3 Hz, 2H), 2.54 (t, J = 6.5 Hz, 2H), 2.26 (s, 3H), 2.11 (s, 3H); LC–MS (ESI): m/z 385 $[M+H]^+$; HRMS (ESI): m/z calcd for $C_{19}H_{21}ClN_6O+H^+$ 385.1538, found 385.1541.

5.1.22. 5-(2-Aminopyrimidin-4-yl)-2-(5-chloro-2-methylphenyl)-*N*-(2-fluoroethyl)-1*H*-pyrrole-3-carboxamide (12)

^{1}H NMR (400 MHz, DMSO-d_6) δ 11.90 (br s, 1H), 8.20 (d, J = 5.2 Hz, 1H), 8.03 (t, J = 5.5 Hz, 1H), 7.38 (d, J = 1.9 Hz, 1H), 7.35 (dd, J = 2.3, 8.3 Hz, 1H), 7.28 (d, J = 2.3 Hz, 1H), 7.28 (d, J = 8.3 Hz, 1H), 6.94 (d, J = 5.2 Hz, 1H), 6.33 (br s, 1H), 4.43 (td, J = 5.2, 47.5 Hz, 2H), 3.44 (q, J = 5.2 Hz, 2H), 2.10 (s, 3H); LC–MS (ESI): m/z 374 $[M+H]^+$; HRMS (ESI): m/z calcd for $C_{18}H_{17}ClFN_5O+H^+$ 374.1179, found 374.1185.

5.1.23. 5-(2-Aminopyrimidin-4-yl)-2-(5-chloro-2-methylphenyl)-*N*-(2-methoxyethyl)-1*H*-pyrrole-3-carboxamide (13)

^{1}H NMR (400 MHz, DMSO-d_6) δ 11.87 (br s, 1H), 8.19 (d, J = 5.2 Hz, 1H), 7.69 (t, J = 5.5 Hz, 1H), 7.36 (dd, J = 2.2, 8.2 Hz, 1H), 7.34 (d, J = 2.6 Hz, 1H), 7.28 (d, J = 2.3 Hz, 1H), 7.29 (d, J = 7.9 Hz, 1H), 6.94 (d, J = 5.2 Hz, 1H), 6.33 (br s, 2H), 3.22 (s, 3H), 2.10 (s, 3H); LC–MS (ESI): m/z 386 $[M+H]^+$; HRMS (ESI): m/z calcd for $C_{19}H_{20}ClN_5O_2+H^+$ 386.1379, found 386.1384.

5.1.24. 5-(2-Aminopyrimidin-4-yl)-2-(5-chloro-2-methylphenyl)-*N*-(2-methylpropyl)-1*H*-pyrrole-3-carboxamide (14)

^{1}H NMR (400 MHz, DMSO-d_6) δ 11.84 (br s, 1H), 8.19 (d, J = 5.2 Hz, 1H), 7.72 (t, J = 5.9 Hz, 1H), 7.35 (dd, J = 2.3, 8.3 Hz, 1H), 7.35 (d, J = 2.3 Hz, 1H), 7.29 (d, J = 2.2 Hz, 1H), 7.28 (d, J = 8.3 Hz, 1H), 6.95 (d, J = 5.2 Hz, 1H), 6.33 (br s, 2H), 2.92 (t, J = 6.4 Hz, 2H), 2.11 (s, 3H), 1.71 (spt, J = 6.8 Hz, 1H), 0.81 (d, J = 6.7 Hz, 6H); LC–MS (ESI): m/z 384 $[M+H]^+$; HRMS (ESI): m/z calcd for $C_{20}H_{22}ClN_5O+H^+$ 384.1586, found 384.1592).

5.1.25. 5-(2-Aminopyrimidin-4-yl)-*N*-benzyl-2-(5-chloro-2-methylphenyl)-1*H*-pyrrole-3-carboxamide (15)

^{1}H NMR (400 MHz, DMSO-d_6) δ 11.89 (br s, 1H), 8.38 (t, J = 6.0 Hz, 1H), 8.20 (d, J = 5.2 Hz, 1H), 7.40 (d, J = 2.6 Hz, 1H), 7.34 (m, 1H), 7.17–7.32 (m, 7H), 6.94 (d, J = 5.2 Hz, 1H), 6.33 (br s, 2H), 4.32 (d, J = 6.1 Hz, 2H), 2.09 (s, 3H); LC–MS (ESI): m/z 418 $[M+H]^+$; HRMS (ESI): m/z calcd for $C_{23}H_{20}ClN_5O+H^+$ 418.1429, found 418.1429.

5.1.26. 5-(2-Aminopyrimidin-4-yl)-2-(5-chloro-2-methylphenyl)-*N*-phenyl-1*H*-pyrrole-3-carboxamide (16)

^{1}H NMR (400 MHz, DMSO-d_6) δ 12.05 (br s, 1H), 9.74 (s, 1H), 8.23 (d, J = 5.2 Hz, 1H), 7.65 (dd, J = 1.0, 8.6 Hz, 2H), 7.57 (d, J = 1.3 Hz, 1H), 7.37 (dd, J = 2.3, 8.0 Hz, 1H), 7.34 (d, J = 2.3 Hz, 1H), 7.30 (d, J = 8.0 Hz, 1H), 7.26 (m, 2H), 7.00 (m, 1H), 6.99 (d, J = 5.2 Hz, 1H), 6.37 (br s, 2H), 2.14 (s, 3H); LC–MS (ESI): m/z 404 $[M+H]^+$; HRMS (ESI): m/z calcd for $C_{22}H_{18}ClN_5O+H^+$ 404.1273, found 404.1274.

5.1.27. 5-(2-Aminopyrimidin-4-yl)-2-(5-chloro-2-methylphenyl)-*N*-(1-methylpiperidin-4-yl)-1*H*-pyrrole-3-carboxamide (17)

^{1}H NMR (400 MHz, DMSO-d_6) δ 11.85 (br s, 1H), 8.19 (d, J = 5.2 Hz, 1H), 7.48 (d, J = 8.2 Hz, 1H), 7.33–7.38 (m, 2H), 7.29 (d, J = 2.0 Hz, 1H), 7.28 (d, J = 8. 7 Hz, 1H), 6.94 (d, J = 5.2 Hz, 1H), 6.32 (br s, 2H), 3.55 (m, 1H), 2.63 (m, 2H), 2.12 (s, 3H), 2.10 (s, 3H), 1.88 (dt, J = 2.1, 11.4 Hz, 2H), 1.65 (m, 2H), 1.45 (dq, J = 3.9, 11.6 Hz, 2H); LC–MS (ESI): m/z 425 $[M+H]^+$; HRMS (ESI): m/z calcd for $C_{22}H_{25}ClN_6O+H^+$ 425.1851, found 425.1846.

5.1.28. 5-(2-Aminopyrimidin-4-yl)-2-(5-chloro-2-methylphenyl)-1-methyl-1*H*-pyrrole-3-carboxamide (18)

To a solution of **38e** (105.2 mg, 0.295 mmol) in DMF (2 mL), Cs_2CO_3 (101 mg, 0.31 mmol) and MeI (28 μL, 0.43 mmol) were added. The mixture was stirred at room temperature for 3 h, the solvent was then removed. EtOAc and water were added to the residue, the layers were separated, the aqueous layer was extracted with EtOAc and the combined organic layers were washed with water, dried over sodium sulfate, filtered and concentrated. The crude material was purified by flash chromatography (DCM/MeOH 98:2) affording ethyl 5-(2-aminopyrimidin-4-yl)-2-(5-chloro-2-methylphenyl)-1-methyl-1*H*-pyrrole-3-carboxylate (**40a**, 74 mg, 68%). ^{1}H NMR (400 MHz, DMSO-d_6) δ 8.20 (d, J = 5.2 Hz, 1H), 7.45 (dd, J = 2.3, 8.4 Hz, 1H), 7.38 (d, J = 8.4 Hz, 1H), 7.30 (d, J = 2.3 Hz, 1H), 7.24 (s, 1H), 6.97 (d, J = 5.2 Hz, 1H), 6.58 (s, 2H), 3.98 (q, J = 7.1 Hz, 2H), 3.67 (s, 3H), 2.00 (s, 3H), 1.00 (t, J = 7.1 Hz, 3H); LC–MS (ESI): m/z 371 $[M+H]^+$; HRMS (ESI): m/z calcd for $C_{19}H_{19}ClN_4O_2+H^+$ 371.1270, found 371.1268.

The intermediate **40a** (70 mg, 0.19 mmol) was treated with 2 N NaOH (1.0 mL) in EtOH (1 mL) under reflux for 3 h. After cooling, a solution of citric acid was added. The resultant precipitate was collected by filtration to give 5-(2-aminopyrimidin-4-yl)-2-(5-chloro-2-methylphenyl)-1-methyl-1*H*-pyrrole-3-carboxylic acid (**41a**, 62 mg, 95%). ^{1}H NMR (400 MHz, DMSO-d_6) δ 8.15 (d, J = 5.2 Hz, 1H), 7.36 (dd, J = 2.2, 8.2 Hz, 1H), 7.31 (d, J = 8.2 Hz, 1H), 7.20 (d, J = 2.1 Hz, 1H), 7.10 (s, 1H), 6.88 (d, J = 5.4 Hz, 1H), 6.47 (s, 2H), 3.61 (s, 3H), 2.02 (s, 3H); LC–MS (ESI): m/z 343 $[M+H]^+$; HRMS (ESI): m/z calcd for $C_{17}H_{15}ClN_4O_2+H^+$ 343.0957, found 343.0966.

To a solution of **41a** (34 mg, 0.1 mmol) in DMF/THF (1:1, 2 mL) and DIPEA (36 μL, 0.2 mmol) was added. EDCI (29 mg, 0.15 mmol) and HOBT·NH_3 (23 mg, 0.15 mmol) were added and the reaction mixture was stirred for 3 h at room temperature. The mixture was dropped into a saturated solution of $NaHCO_3$ and ice and extracted with DCM. The combined organic layers were washed with water, dried over sodium sulfate, filtered and concentrated. The crude material was purified by flash chromatography (DCM/MeOH 95:5) affording **18** (21 mg, 63%). ^{1}H NMR (400 MHz, DMSO-d_6) δ 8.21 (d, J = 5.4 Hz, 1H), 7.40 (dd, J = 2.2, 8.2 Hz, 1H), 7.33 (s, 1H), 7.35 (d, J = 8.3 Hz, 1H), 7.23 (d, J = 2.2 Hz, 1H), 7.04 (br s, 1H), 6.81 (d, J = 5.4 Hz, 1H), 6.71 (br s, 1H), 6.54 (s, 2H), 3.61 (s, 3H), 2.00 (s, 3H); LC–MS (ESI): m/z 342 $[M+H]^+$; HRMS (ESI): m/z calcd for $C_{17}H_{16}ClN_5O+H^+$ 342.1116, found 342.1122.

The following compound **19** was prepared according to the method described above using ethyl bromide instead of methyl iodide.

5.1.29. 5-(2-Aminopyrimidin-4-yl)-2-(5-chloro-2-methylphenyl)-1-ethyl-1*H*-pyrrole-3-carboxamide (19)

^{1}H NMR (400 MHz, DMSO-d_6) δ 8.20 (d, J = 5.2 Hz, 1H), 7.41 (dd, J = 2.2, 8.2 Hz, 1H), 7.36 (s, 2H), 7.35 (d, J = 8.2 Hz, 1H), 7.25 (d, J = 2.3 Hz, 1H), 7.03 (br s, 1H), 6.81 (d, J = 5.4 Hz, 1H), 6.70 (br s, 1H), 6.52 (s, 2H), 4.43 (qd, J = 6.9, 13.5 Hz, 1H), 4.00 (qd, J = 6.9, 13.5 Hz, 1H), 2.01 (s, 3H), 0.99 (t, J = 6.9 Hz, 3H); LC–MS (ESI): m/z 356 [M+H]$^+$; HRMS (ESI): m/z calcd for $C_{18}H_{18}ClN_5O$+H$^+$ 356.1273, found 356.1271.

5.1.30. 2-(5-Chloro-2-methylphenyl)-5-(2-{[4-(4-methylpiperazin-1-yl)phenyl]amino}pyrimidin-4-yl)-1*H*-pyrrole-3-carboxamide (23)

To a well stirred suspension of **38e** (416 mg, 1.16 mmol) in THF (15 mL) maintained in an inert atmosphere of argon, cesium iodide (302 mg, 1.16 mmol), iodine (296 mg, 0.58 mmol), copper(I) iodide (74 mg, 0.39 mmol) and *iso*-pentyl nitrite (0.236 mL, 1.75 mmol) were added. The reaction mixture was stirred vigorously under reflux for 2 h. After cooling, the reaction mixture was concentrated to small volume, poured into water (100 mL) and extracted with DCM (5 × 20 mL). The combined organic layers were washed with 33% ammonium hydroxide (2 × 10 mL), 5% solution of sodium thiosulphate (2 × 50 mL), brine (2 × 20 mL) and dried over anhydrous sodium sulfate, filtered and concentrated. The crude material was purified by flash chromatography (EtOAc/hexane 40:60) affording ethyl 2-(5-chloro-2-methylphenyl)-5-(2-iodopyrimidin-4-yl)-1*H*-pyrrole-3-carboxylate (**42a**, 130 mg, 24%). ^{1}H NMR (400 MHz, DMSO-d_6) δ 12.58 (br s, 1H), 8.43 (d, J = 5.4 Hz, 1H), 7.91 (d, J = 5.4 Hz, 1H), 7.53 (d, J = 2.7 Hz, 1H), 7.41–7.45 (m, 1H), 7.32–7.36 (m, 2H), 4.05 (m, 2H), 2.11 (s, 3H), 1.10 (m, 3H); LC–MS (ESI): m/z 467 [M+H]$^+$; HRMS (ESI): m/z calcd for $C_{18}H_{15}ClIN_3O_2$+H$^+$ 467.9971, found 467.9966.

Pd(OAc)$_2$ (5.5 mg, 0.025 mmol), (±)-BINAP (15.5 mg, 0.025 mmol) and DMF (5 mL) were charged in a round-bottom flask flushed with argon. The flask was evacuated and backfilled with argon. The mixture was stirred under argon for 30 min and **42a** (117 mg, 0.25 mmol), 4-(4-methyl-piperazin-1-yl)-phenylamine (143 mg, 0.75 mmol), potassium carbonate (518 mg, 3.75 mmol) were added. The flask was evacuated and backfilled with argon. The resulting mixture was stirred at 80 °C for 3 h under argon. After cooling to room temperature, the reaction mixture was filtered on a pad of celite. The solvent was concentrated, the crude solid was purified by flash chromatography on silica gel (DCM/MeOH 90:10) to afford ethyl 2-(5-chloro-2-methylphenyl)-5-(2-{[4-(4-methylpiperazin-1-yl)phenyl]amino}pyrimidin-4-yl)-1*H*-pyrrole-3-carboxylate (**43a**, 40 mg, 30%). ^{1}H NMR (400 MHz, DMSO-d_6) δ 12.24 (d, J = 2.2 Hz, 1H), 9.15 (s, 1H), 8.38 (d, J = 5.2 Hz, 1H), 7.63 (d, J = 9.0 Hz, 2H), 7.42 (dd, J = 2.3, 8.2 Hz, 1H), 7.35 (d, J = 8.2 Hz, 1H), 7.33–7.39 (m, 2H), 7.16 (d, J = 5.2 Hz, 1H), 6.89 (d, J = 9.1 Hz, 2H), 4.06 (q, J = 7.0 Hz, 2H), 3.07 (m, 4H), 2.46 (m, 4H), 2.22 (s, 3H), 2.14 (s, 3H), 1.09 (t, J = 7.1 Hz, 3H); LC–MS (ESI): m/z 531 [M+H]$^+$; HRMS (ESI): m/z calcd for $C_{29}H_{31}ClN_6O_2$+H$^+$ 531.2270, found 531.2274.

The carboxylate **43a** (35 mg, 0.06 mmol) was treated with 2 N NaOH (0.3 mL) in EtOH (1 mL) under reflux for 3 h. After cooling, acetic acid was added and after centrifugation, the resultant precipitate was collected by filtration to give 2-(5-chloro-2-methylphenyl)-5-(2-{[4-(4-methylpiperazin-1-yl)phenyl]amino}pyrimidin-4-yl)-1*H*-pyrrole-3-carboxylic acid (**44a**), which was used directly in the next synthetic step.

A solution of the crude **44a** in DMF/THF (1:1, 1 mL) and DIPEA (46 μL, 0.26 mmol) was stirred at 0 °C. EDCI (25 mg, 0.13 mmol) and HOBT·NH$_3$ (10 mg, 0.13 mmol) were added and the reaction mixture was stirred for 3 h at room temperature. THF was evaporated, the mixture was dropped into a saturated solution of NaHCO$_3$ and extracted with DCM/MeOH (9:1, 5 × 5 mL). The combined organic layers were washed with water, dried over Na$_2$SO$_4$, filtered and concentrated. The crude material was purified by flash chromatography (DCM/MeOH 9:1) affording **23** (21 mg, 70%, 2 steps). ^{1}H NMR (400 MHz, DMSO-d_6) δ 11.90 (d, J = 2.2 Hz, 1H), 9.11 (s, 1H), 8.35 (d, J = 5.2 Hz, 1H), 7.68 (d, J = 9.0 Hz, 2H), 7.41 (d, J = 2.7 Hz, 1H), 7.37 (dd, J = 2.3, 8.2 Hz, 1H), 7.29–7.34 (m, 2H), 7.10 (d, J = 5.2 Hz, 1H), 6.91 (d, J = 9.1 Hz, 2H), 6.79 (br s, 1H), 3.07 (m, 4H), 2.47 (m, 4H), 2.23 (s, 3H), 2.15 (s, 3H); LC–MS (ESI): m/z 502 [M+H]$^+$; HRMS (ESI): m/z calcd for $C_{27}H_{28}ClN_7O$+H$^+$ 502.2117, found 502.2118.

The following compound **24** was prepared according to the method described above starting from **40a**.

5.1.31. 2-(5-Chloro-2-methylphenyl)-1-methyl-5-(2-{[4-(4-methylpiperazin-1-yl)phenyl]amino}pyrimidin-4-yl)-1*H*-pyrrole-3-carboxamide (24)

^{1}H NMR (400 MHz, DMSO-d_6) δ 9.19 (s, 1H), 8.37 (d, J = 5.2 Hz, 1H), 7.51 (m, 2H), 7.40–7.44 (m, 2H), 7.37 (m, 1H), 7.26 (d, J = 2.3 Hz, 1H), 7.08 (br s, 1H), 6.99 (d, J = 5.2 Hz, 1H), 6.88 (m, 2H), 6.75 (br s, 1H), 3.62 (s, 3H), 3.05 (m, 4H), 2.44 (m, 4H), 2.22 (s, 3H), 2.01 (s, 3H); LC–MS (ESI): m/z 516 [M+H]$^+$; HRMS (ESI): m/z calcd for $C_{28}H_{30}ClN_7O$+H$^+$ 516.2273, found 516.2273.

5.1.32. 2-(5-Chloro-2-methylphenyl)-5-(pyrimidin-4-yl)-1*H*-pyrrole-3-carboxamide (20)

Potassium *tert*-pentoxide 1.7 M in toluene (86.4 mL, 147.9 mmol) was added drop wise to a solution of methyl 5-chloro-2-methylbenzoate (**45**, 18.2 g, 98.6 mmol) and acetonitrile (15.4 mL, 296 mmol) in anhydrous toluene (150 mL). The mixture was stirred at room temperature for 20 min, then diluted with 1 N HCl (60 mL), and extracted with EtOAc (3 × 150 mL). The organic layer was collected, washed with water and brine, dried over sodium sulfate and concentrated. Column chromatography on silica gel (0–20% EtOAc/hexane) provided 3-(5-chloro-2-methylphenyl)-3-oxopropanenitrile (**46**, 13.7 g, 72%). ^{1}H NMR (400 MHz, DMSO-d_6) δ 7.88 (d, J = 2.1 Hz, 1H), 7.57 (dd, J = 1.9, 8.4 Hz, 1H), 7.38 (m, 1H), 4.69 (s, 2H), 2.41 (s, 3H); GC–MS (EI): m/z 193.0294; HRMS (ESI): m/z calcd for $C_{10}H_8ClNO$+Na$^+$ 216.0186, found 216.0184.

A mixture of **46** (13.0 g, 67.1 mmol), aminoacetaldehyde diethyl acetal (11.7 mL, 80.5 mmol) and toluene (150 mL) was stirred under reflux for 5 h under nitrogen atmosphere in the Dean-Stark apparatus. The mixture was evaporated in vacuo and added to TFA (50 mL) at 5 °C. After stirring at room temperature for 30 min, the reaction mixture was concentrated and then diluted with EtOAc and saturated solution of sodium hydrogen carbonate. The organic layer was separated, washed with water and brine, dried over sodium sulfate and concentrated. Column chromatography on silica gel (0–20% EtOAc/hexane) afforded 2-(5-chloro-2-methylphenyl)-1*H*-pyrrole-3-carbonitrile (**47**, 8.1 g, 56%, 2 steps). ^{1}H NMR (400 MHz, DMSO-d_6) δ 11.99 (br s, 1H), 7.34–7.47 (m, 2H), 7.38 (d, J = 2.2 Hz, 1H), 7.04 (t, J = 2.8 Hz, 1H), 6.59 (t, J = 2.6 Hz, 1H), 2.26 (s, 3H); LC–MS (ESI): m/z 217 [M+H]$^+$; HRMS (ESI): m/z calcd for $C_{12}H_9ClN_2$+H$^+$ 217.0527, found 217.0526.

To a mixture of **47** (1.80 g, 8.28 mmol) in DCM (40 mL) was added acetyl chloride (0.936 mL, 13.14 mmol) at room temperature, under nitrogen. The resultant mixture was cooled to 0 °C and anhydrous aluminum trichloride (2.62 g, 19.8 mmol) was added in small portions during a period of 10 min, keeping the internal temperature below 5 °C. Upon complete addition, the mixture was brought to room temperature and allowed to stir for 30 min. Then, the mixture was slowly poured in a solution of ice-cooled 1 N HCl solution (18 mL). The aqueous layer was separated and extracted twice with DCM (40 mL). The combined organic

extracts were washed with brine, dried over sodium sulfate and concentrated under reduced pressure. The crude material was chromatographed on silica gel (10–20% EtOAc/hexane) to afford 5-acetyl-2-(5-chloro-2-methylphenyl)-1*H*-pyrrole-3-carbonitrile (**48**, 2.0 g, 86%). ^{1}H NMR (400 MHz, DMSO-d_6) δ 12.89 (br s, 1H), 7.60 (d, J = 2.4 Hz, 1H), 7.49 (dd, J = 2.4, 8.4 Hz, 1H), 7.43 (d, J = 2.3 Hz, 1H), 7.42 (d, J = 8.4 Hz, 1H), 2.43 (s, 3H), 2.24 (s, 3H); LC–MS (ESI): m/z 259 $[M+H]^+$; HRMS (ESI): m/z calcd for $C_{14}H_{11}ClN_2O+Na^+$ 281.0452, found 281.0452.

To a suspension of **48** (225 mg, 0.87 mmol) in DMF (2.5 mL) was added *N*,*N*-dimethylformamide diisopropyl acetal (0.54 mL, 2.61 mmol). The mixture was allowed to stir overnight at 90 °C, evaporated in vacuo, suspended in DMF (2.5 mL) and treated with formamidine acetate (208 mg, 2.0 mmol). The mixture was heated to 150 °C for 5 h under efficient stirring. The resulting mixture was diluted by drop wise addition of water and extracted with EtOAc. The organic phase was washed with brine, water and then dried over sodium sulfate and concentrated. The crude material was chromatographed on silica gel (hexane/EtOAc 90:10) to afford 2-(5-chloro-2-methylphenyl)-5-(pyrimidin-4-yl)-1*H*-pyrrole-3-carbonitrile (**50**, 77 mg, 30%, 2 steps). ^{1}H NMR (400 MHz, DMSO-d_6) δ 12.98 (br s, 1H), 9.13 (d, J = 1.2 Hz, 1H), 8.79 (d, J = 5.4 Hz, 1H), 7.90 (dd, J = 1.3, 5.4 Hz, 1H), 7.61 (s, 1H), 7.48 (m, 2H), 7.43 (m, 1H), 2.30 (s, 3H); LC–MS (ESI): m/z 295 $[M+H]^+$; HRMS (ESI): m/z calcd for $C_{16}H_{11}ClN_4+H^+$ 295.0745, found 295.0750.

To a solution of **50** (67 mg, 0.23 mmol) in TFA (1.0 mL) were sequentially added water (0.15 mL) and 98% sulfuric acid (0.30 mL) under efficient stirring. The mixture was allowed to stir for 5 h at 70 °C and then was diluted by drop wise addition of water (1 mL). The reaction mixture was made basic (pH 10-12) by adding 30% aqueous ammonia (3 mL) under stirring. The precipitated solid was collected by filtration, washed with water and finally dried in a vacuum oven at 50 °C affording **20** (72 mg, 83%).

^{1}H NMR (400 MHz, DMSO-d_6) δ 12.22 (br s, 1H), 9.04 (d, J = 1.1 Hz, 1H), 8.70 (d, J = 5.5 Hz, 1H), 7.74 (dd, J = 1.4, 5.4 Hz, 1H), 7.57 (d, J = 2.7 Hz, 1H), 7.36 (m, 1H), 7.12–7.33 (m, 3H), 6.81 (br s, 1H), 2.13 (s, 3H); LC–MS (ESI): m/z 313 $[M+H]^+$; HRMS (ESI): m/z calcd for $C_{16}H_{13}ClN_4O+H^+$ 313.0851, found 313.0853.

5.1.33. 2-(5-Chloro-2-methylphenyl)-5-[2-(methylamino)pyrimidin-4-yl]-1*H*-pyrrole-3-carboxamide (21)

To a suspension of **48** (225 mg, 0.87 mmol) in DMF (2.5 mL) was added *N*,*N*-dimethylformamide diisopropyl acetal (0.54 mL, 2.61 mmol). The mixture was allowed to stir overnight at 90 °C, evaporated in vacuo, suspended in DMF (2.5 mL) and treated with methylguanidine hydrochloride (115 mg, 1.05 mmol) and K_2CO_3 (159 mg, 1.14 mmol). The mixture was heated to 110 °C for 5 h under efficient stirring. The resulting mixture was concentrated and chromatographed on silica gel (10–30% EtOAc/hexane) to afford 2-(5-chloro-2-methylphenyl)-5-[2-(methylamino)pyrimidin-4-yl]-1*H*-pyrrole-3-carbonitrile (**51**, 135 mg, 48%, 2 steps). ^{1}H NMR (400 MHz, DMSO-d_6) δ 12.53 (br s, 1H), 8.27 (d, J = 4.6 Hz, 1H), 7.46–7.53 (m, 3H), 7.44 (m, 1H), 7.38 (m, 1H), 6.98 (d, J = 5.2 Hz, 1H), 6.91 (br s, 1H), 2.88 (d, J = 4.5 Hz, 3H) 2.28 (s, 3H); LC–MS (ESI): m/z 324 $[M+H]^+$; HRMS (ESI): m/z $C_{17}H_{14}ClN_5+H^+$ 324.1011, found 324.1013.

To a solution of **51** (74 mg, 0.23 mmol) in TFA (1.0 mL) were sequentially added water (0.15 mL) and 98% sulfuric acid (0.30 mL) under efficient stirring. The mixture was allowed to stir for 8 h at 70 °C and then was diluted by drop wise addition of water (3 mL). The reaction mixture was made basic (pH 10-12) by adding 30% aqueous ammonia (1 mL) under stirring. The precipitated solid was collected by filtration, washed with water and finally dried in a vacuum oven at 50 °C affording **21** (66 mg, 88%).

^{1}H NMR (400 MHz, DMSO-d_6) δ 11.87 (br s, 1H), 8.20 (d, J = 5.4 Hz, 1H), 7.39 (s, 1H), 7.34–7.38 (m, 1H), 7.26–7.32 (m, 2H), 7.19 (br s, 1H), 6.88 (d, J = 5.1 Hz, 1H), 6.67–6.83 (m, 1H), 2.88 (d, J = 4.1 Hz, 3H), 2.12 (s, 3H); LC–MS (ESI): m/z 342 $[M+H]^+$; HRMS (ESI): m/z calcd for $C_{17}H_{16}ClN_5O+H^+$ 342.1116, found 342.1118.

5.1.34. 2-(5-Chloro-2-methylphenyl)-5-{2-[(4-methoxybenzyl)amino]pyrimidin-4-yl}-1*H*-pyrrole-3-carboxamide (22)

To a suspension of **48** (225 mg, 0.87 mmol) in DMF (2.5 mL) was added *N*,*N*-dimethylformamide diisopropyl acetal (0.54 mL, 2.61 mmol). The mixture was allowed to stir overnight at 90 °C, evaporated in vacuo, suspended in DMF (2.5 mL) and treated with guanidine carbonate (127 mg, 1.05 mmol). The mixture was heated to 110 °C for 5 h under efficient stirring. The resulting mixture was concentrated and chromatographed on silica gel (10–30% EtOAc/hexane) to afford 5-(2-aminopyrimidin-4-yl)-2-(5-chloro-2-methylphenyl)-1*H*-pyrrole-3-carbonitrile (**49**, 148 mg, 55%, 2 steps). ^{1}H NMR (400 MHz, DMSO-d_6) δ 12.79 (br s, 1H), 8.30 (d, J = 5.7 Hz, 1H), 7.46–7.54 (m, 3H), 7.44 (m, 1H), 7.14 (d, J = 5.7 Hz, 1H), 7.05 (br s, 1H), 2.28 (s, 3H); LC–MS (ESI): m/z 310 $[M+H]^+$; HRMS (ESI): m/z calcd for $C_{16}H_{12}ClN_5+H^+$ 310.0854, found 310.0853.

To a solution of **49** (142 mg, 0.46 mmol) in TFA (2.0 mL) were sequentially added water (0.3 mL) and 98% sulfuric acid (0.6 mL) under efficient stirring. The mixture was allowed to stir for 8 h at 70 °C and then was diluted by drop wise addition of water (6 mL). The reaction mixture was made basic (pH 10-12) by adding 30% aqueous ammonia (2 mL) under stirring. The precipitated solid was collected by filtration, washed with water and finally dried in a vacuum oven at 50 °C affording **6** (128 mg, 85%).

To a stirred solution of **6** (100 mg, 0.305 mmol), TFA (0.28 mL, 3.66 mL) and 4-methoxybenzaldehyde (0.074 mL, 0.61 mmol) in DMF (2 mL) was added portionwise sodium triacetoxyborohydride (129 mg, 0.61 mmol). After stirring at room temperature overnight, the solution was taken up in EtOAc and thoroughly washed with brine. After drying over sodium sulfate, the solvent was removed and the residue was purified by flash chromatography (DCM/MeOH, 96:4) to provide **22** (86 mg, 63%). ^{1}H NMR (400 MHz, DMSO-d_6) δ 11.84 (br s, 1H), 8.19 (d, J = 5.2 Hz, 1H), 7.39 (d, J = 2.4 Hz, 1H), 7.26–7.40 (m, 7H), 7.19 (br s, 1H), 6.84 (d, J = 8.8 Hz, 2H), 6.78 (br s, 1H), 4.55 (d, J = 4.1 Hz, 2H), 3.70 (s, 3H), 2.13 (s, 3H); LC–MS (ESI): m/z 448 $[M+H]^+$; HRMS (ESI): m/z calcd for $C_{24}H_{22}ClN_5O_2+H^+$ 448.1535, found 448.1543.

5.2. Crystallographic methods

Crystallization studies were performed using a construct encompassing the C-terminal kinase domain (aa 835-1132). Crystals of the kinase domain of JAK2 in complex with compounds **6**, **24** and **28** were grown from a solution of 1.5–2.2 M sodium malonate pH 7. The protein was concentrated at 10 mg/mL and compound was added to a nominal concentration of 1 mM. For data collection, the crystals were transferred to drops containing the equivalent mother liquor with 20% glycerol. Diffraction data for compounds **6** and **28** were collected at the ESRF (Grenoble, France) on beamlines ID23-1 and ID29, respectively, while diffraction data for compound **24** were collected in house using a Rigaku Micromax-007 HF X-ray generator and Mar345 Image Plate Detector (Marresearch). Data were processed using the HKL2000 package.[29] The three structures were solved by molecular replacement with Phaser[30] using a published structure of JAK2 (PDB code 2B7A) as a search model. Model building was done using Coot[31] and refinement was done with RefMac.[32] The coordinates and the corresponding structure factors were deposited in the Protein Data Bank with code 4D0W, 4D1S and 4D0X for **6**, **24** and **28**, respectively.

5.3. Biochemical assay

Enzyme assays were performed using a radiometric assay in which specific JAK2, JAK1, JAK3 and TYK2 peptide substrates are *trans*-phosphorylated by JAK kinases in the presence of ATP traced with 33P-γ-ATP and recombinant epitope tagged kinase domains JAK2 (residues 808-1132, Invitrogen, Eugene, OR), JAK1 (residues 861-1152, P23458 UniProtKB/Swiss-Prot), JAK3 (residues 781-1124, P52333 UniProtKB/Swiss-Prot) and TYK2 (residues 833-1187, P29597 UniProtKB/Swiss-Prot). The kinase assays were run with a final enzyme concentration of 1 nM for JAK2 and JAK3, 2.5 nM for JAK1 and 3 nM for TYK2. On the contrary of the other JAKs, an auto-phosphorylation step was requested for JAK1, due to not linear kinase reaction (1 μM JAK1 in presence of 750 μM ATP was kept at 28 °C for 60 min). After this preactivation step the JAK1 kinetic resulted linear over time. The peptidic substrate LPLDKDYYVVREPGQ was used at 64 and 40 μM for JAK2 and JAK3, respectively. The peptididic substrate KKHTDDGYMPMSPGVA was used at 154 and 71 μM for JAK1 and TYK2, respectively. The ATP, in the presence of 1–2 nM 33P-γ-ATP, was used at concentration twofold the αKm for each enzyme. The reaction was performed in 50 mM HEPES pH 7.5 containing 10 mM $MgCl_2$, 2.5 mM DTT, 10 μM Na_3VO_4 and 0.2 mg/mL BSA. At the end of the kinase reaction, all the unreacted ATP is captured by an excess of Dowex ion-exchange resins (SIGMA, DOWEX 1 × 8, 200–400 mesh) previously prepared by three overnight washes with 150 mM sodium formate, pH 3.0. The supernatant is subsequently withdrawn and transferred into a counting plate and analysed by β-counting. Data per each compound was analyzed by an internally customized version of the SW package 'Assay Explorer' which provides sigmoidal fittings of the ten dilution curves for IC_{50} determination.

Selectivity against other kinases was evaluated on an internally developed Kinase Selectivity Screening (KSS) panel, designed to represent the overall diversity of the kinome, as described in detail in a recent publication.[33] The panel includes: ABL, ACK1, AKT1, Alk, AUR1, AUR2, BRK, CDC7, CDK2/CYCA, CHK1, CK2alpha/beta, eEF2K, EGFR1, ERK2, FAK, FGFR1, Flt3, GSK3beta, Haspin V473-K798, IGFR1, IKK2, IR, JAK1, JAK2, JAK3, KIT, LCK, MELK, MET, MK2, MPS1, MST4, NEK6, NIM, P38alpha, PAK4, PDGFRb, PDK1, PERK, PIM1, PIM2, PKAalpha, PKCbetaII, PLK1, RET, SULU1, SYK, TRKA, TYK2, VEGFR2, VEGFR3, ZAP70.

5.4. Cells proliferation assay

JAK2 dependent human megakaryoblastic leukemia SET-2 cell line (DSMZ, Braunschweig GERMANY), human IL-2 dependent T cell lymphoma DERL-7 cell line (DSMZ, Braunschweig GERMANY) and human ovarian carcinoma A2780 (ECACC, Salisbury, UK) were cultured in RPMI 1640 medium Glutamax (Gibco BRL, Gaithesburg, MD, USA), supplemented with 10% fetal bovine serum (FBS) at 37 °C and 5% CO_2. Human IL-2 (20 ng/ml, Sigma-Aldrich, St. Louis, MO) was added at medium for DERL-7. Approximately 5×10^3 cells were plated into 384 microtiter plate wells in 50 μL of growth media with different concentrations of inhibitors. The cells were incubated at 37 °C and 5% CO_2 for 72 h, then the plates were processed using Cell Titer-Glo assay (Promega, Madison, WI, USA), following the manufacturer's instruction. Briefly, 25 μL/well reagent solution is added to each well and after 5 min shacking micro-plates are read by Envision luminometer (PerkinElmer, Waltham, MA, USA). Data are analyzed by Symix Assay Explorer software (Symix Technologies Inc.) that provides sigmoidal fitting algorithm of the 8 points dilutions curves for IC_{50} determination.

5.5. Biomarker evaluation in cells

For the mechanism of action the SET-2 cell line was treated with compound at the indicated concentration for 2 h at 37 °C or with just DMSO as a control. DERL-7 cell line was starved for 18 h and then treated with the compound for 2 h before activation with human IL-2 (20 ng/ml, 15 min at 37 °C). At the end of treatment both the cell lines were centrifuged, washed with cold PBS and lysed in RIPA buffer. The lysates were centrifuged at 13,000 rpm for 15 min at 4 °C. Equal amounts of cell lysates were resolved by SDS–PAGE and then transferred to Wathman Nitrocellulose transfer membrane (GE Healthcare UK Limited, Buckinghamshire, UK). The membranes were incubated in blocking solution consisting of 5% powered milk in TBST at room temperature for 1 h and then overnight at 4 °C with the antibodies specific for P-STAT5, P-STAT3, STAT5 and STAT3 total protein (Cell Signaling Technology, Danvers, MA). Protein bands were visualised by using an enhanced chemiluminescence detection system (Liteablot® Plus, Euroclone, Milan, Italy) and autoradiography.

5.6. High throughput solubility

Solubility at pH 7 was performed as previously described.[34]

5.7. In vivo pharmacokinetics

The pharmacokinetic profiles of compounds were investigated in overnight fasted male Nu/Nu mice following a single dose given intravenously (iv) and orally (po). The vehicle used was 10% Tween 80 in 5% dextrose solution for iv administration and 0.5% methocel for os administration. A total of three mice were treated for each administration. Blood samples of each mouse were collected from the saphenous vein at predose, 0.083, 0.5, 1, 6, and 24 h postdosing. Samples were centrifuged at 10,000*g* for 3 min at 4 °C and the plasma was stored at −80 °C until analysis. Samples were analyzed by LC/MS/MS technique.

5.8. In vivo pharmacology

Acute megakaryoblastic leukemia cell line SET-2 (10^7 cells) was inoculated s.c. in 5–6 weeks old female severe combined immunodeficient (SCID) mice (Charles River) previously exposed to gamma irradiation (200 Rads of whole body gamma irradiation). Mice bearing a palpable tumour (100–200 mm^3) were treated with the vehicle (0.5% methocel) or the compound. Tumour dimensions were measured regularly using Vernier calipers and tumour volume was calculated according to the following formula: tumour volume (mm^3) = length × width^2/2. The tumour growth inhibition (% TGI) was calculated according to the equation: % TGI = 100 − (Mean tumour volume of treated group/Mean tumour volume of control group) × 100. All procedures adopted for housing and handling of animals were in strict compliance with Italian and European guidelines for Laboratory Animal Welfare.

For in vivo mechanism of action studies, mice bearing tumour were treated with single dose of compound and sacrificed at different post treatment times (3 animals/time), the tumours were lysed and analyzed by Western Blot as described for cells.

Acknowledgments

We thank Nicoletta Colombo for skillful assistance in NMR spectra recording and interpretation, Nadia Amboldi and the group of Cell Screening for cell proliferation assay, and the Experimental Therapy group for in vivo experiments.

Supplementary data

Supplementary data associated with this article can be found, in the online version, at http://dx.doi.org/10.1016/j.bmc.2014.06.025.

References and notes

1. Parganas, E.; Wang, D.; Stravopodis, D.; Topham, D. J.; Marine, J. C.; Teglund, S.; Vanin, E. F.; Bodner, S.; Colamonici, O. R.; van Deursen, J. M.; Grosveld, G.; Ihle, J. N. *Cell* **1998**, *93*, 385.
2. Park, S. O.; Wamsley, H. L.; Bae, K.; Hu, Z.; Li, X.; Choe, S. W.; Slayton, W. B.; Oh, S. P.; Wagner, K. U.; Sayeski, P. P. *PLoS One* **2013**, *8*, e59675.
3. Ihle, J. N.; Gilliland, D. G. *Curr. Opin. Genet. Dev.* **2007**, *17*, 8.
4. O'Shea, J. J.; Gadina, M.; Schreiber, R. D. *Cell* **2002**, *109*, S121.
5. Dawson, M. A.; Bannister, A. J.; Gòttgens, B.; Foster, S. D.; Bartke, T.; Green, A. R.; Kouzarides, T. *Nature* **2009**, *46*, 819.
6. (a) Levine, R. L.; Belisle, C.; Wadleigh, M.; Zahrieh, D.; Lee, S.; Chagnon, P.; Gilliland, D. G.; Busque, L. *Blood* **2006**, *107*, 4139; (b) Baxter, E. J.; Scott, L. M.; Campbell, P. J.; East, C.; Fourouclas, N.; Swanton, S.; Vassiliou, G. S.; Bench, A. J.; Boyd, E. M.; Curtin, N.; Scott, M. A.; Erber, W. N.; Green, A. R. *Lancet* **2005**, *365*, 1054; (c) Kralovics, R.; Passamonti, F.; Buser, A. S.; Teo, S. S.; Tiedt, R.; Passweq, J. R.; Tichelli, A.; Cazzola, M.; Skoda, R. C. *N. Eng. J. Med.* **2005**, *352*, 1779.
7. Levine, R. L.; Pardanani, A.; Tefferi, A.; Gilliland, D. G. *Nat. Rev. Cancer* **2007**, *7*, 673.
8. O'Shea, J. J.; Holland, S. M.; Staudt, L. M. *N. Eng. J. Med.* **2013**, *368*, 161.
9. LaFave, L. M.; Levine, R. L. *Trends Pharmacol. Sci.* **2012**, *33*, 574.
10. (a) Kiss, R.; Sayeski, P. P.; Keseru, G. M. *Expert Opin. Ther. Patents* **2010**, *20*, 471; (b) Baskin, R.; Majumder, A.; Sayeski, P. P. *Curr. Med. Chem.* **2010**, *17*, 4551; (c) Dymock, B. W.; See, C. S. *Expert Opin. Ther. Patents* **2013**, *23*, 449.
11. (a) Lucia, E.; Recchia, A. G.; Gentile, M.; Bossio, S.; Vigna, E.; Mazzone, C.; Madeo, A.; Morabito, L.; Gigliotti, V.; deStefano, L.; Caruso, N.; Servillo, P.; Franzese, S.; Bisconte, M. G.; Gentile, C.; Morabito, F. *Expert Opin. Invest. Drugs* **2011**, *20*, 41; (b) Tam, C. S.; Verstovsek, S. *Expert Opin. Invest. Drugs* **2013**, *22*, 687.
12. Pardanani, A.; Gotlib, J. R.; Jamieson, C.; Cortes, J. E.; Talpaz, M.; Stone, R. M.; Silverman, M. H.; Gilliland, D. G.; Shorr, J.; Tefferi, A. *J. Clin. Oncol.* **2011**, *29*, 789.
13. Santos, F. P.; Kantarjian, H. M.; Jain, N.; Manshouri, T.; Thomas, D. A.; Garcia-Manero, G.; Kennedy, D.; Estrov, Z.; Cortes, J.; Verstovsek, S. *Blood* **2010**, *115*, 1131.
14. Tyner, J. W.; Bumm, T. G.; Deininger, J.; Wood, L.; Aichberger, K. J.; Loriaux, M. M.; Druker, B. J.; Burns, C. J.; Fantino, E.; Deininger, M. W. *Blood* **2010**, *115*, 5232.
15. Hart, S.; Goh, K. C.; Novotny-Diermayr, V.; Hu, C. Y.; Hentze, H.; Tan, Y. C.; Madan, B.; Amalini, C.; Loh, Y. K.; Ong, L. C.; William, A. D.; Lee, A.; Poulsen, A.; Jayaraman, R.; Ong, K. H.; Ethirajulu, K.; Dymock, B. W.; Wood, J. W. *Leukemia* **2011**, *25*, 1751.
16. Ma, L.; Clayton, J. R.; Walgren, R. A.; Zhao, B.; Evans, R. J.; Smith, M. C.; Heinz-Taheny, K. M.; Kreklau, E. L.; Bloem, L.; Pitou, C.; Shen, W.; Strelow, J. M.; Halstead, C.; Rempala, M. E.; Parthasarathy, S.; Gillig, J. R.; Heinz, L. J.; Pei, H.; Wang, Y.; Stancato, L. F.; Dowless, M. S.; Iversen, P. W.; Burkholder, T. P. *Blood Cancer J.* **2013**, *3*, 109.
17. Purandare, A. V.; McDevitt, T. M.; Wan, H.; You, D.; Penhallow, B.; Han, X.; Vuppugalla, R.; Zhang, Y.; Ruepp, S.; Trainor, G. L.; Lombardo, L.; Pedicord, D.; Gottardis, M. M.; Ross-Macdonald, P.; de Silva, H.; Hosbach, J.; Emanuel, S. L.; Blat, Y.; Fitzpatrick, E.; Taylor, T. L.; McIntyre, K. W.; Michaud, E.; Mulligan, C.; Lee, F. Y.; Woolfson, A.; Lasho, T. L.; Pardanani, A.; Tefferi, A.; Lorenzi, M. V. *Leukemia* **2012**, *26*, 280.
18. Ioannidis, S.; Lamb, M. L.; Wang, T.; Almeida, L.; Block, M. H.; Davies, A. M.; Peng, B.; Su, M.; Zhang, H.-J.; Hoffmann, E.; Rivard, C.; Green, I.; Howard, T.; Pollard, H.; Read, J.; Alimzhanov, M.; Bebernitz, G.; Bell, K.; Ye, M.; Huszar, D.; Zinda, M. *J. Med. Chem.* **2011**, *54*, 262.
19. Verstovsek, S.; Kantarjian, H.; Mesa, R. A.; Pardanani, A. D.; Cortes-Franco, J.; Thomas, D. A.; Estrov, Z.; Fridman, J. S.; Bradley, E. C.; Erickson-Viitanen, S.; Vaddi, K.; Levy, R.; Tefferi, A. *N. Eng. J. Med.* **2010**, *363*, 1117.
20. Ostojic, A.; Vrhovac, R.; Verstovsek, S. *Ther. Clin. Risk Manag.* **2012**, *8*, 95.
21. (a) Williams, N. K.; Bamert, R. S.; Patel, O.; Wang, C.; Walden, P. M.; Wilks, A. F.; Fantino, E.; Rossjohn, J.; Lucet, I. S. *J. Mol. Biol.* **2009**, *387*, 219; (b) Chrencik, J. E.; Patny, A.; Leung, I. K.; Korniski, B.; Emmons, T. L.; Hall, T.; Weinberg, R. A.; Gormley, J. A.; Williams, J. M.; Day, J. E.; Hirsch, J. L.; Kiefer, J. R.; Leone, J. W.; Fischer, D.; Sommers, C. D.; Huang, H.-C.; Jacobsen, E. J.; Tenbrink, R. E.; Tomasselli, A. G.; Benson, T. E. *J. Mol. Biol.* **2010**, *400*, 413; (c) Boggon, T. J.; Li, Y.; Manley, P. M.; Eck, M. J. *Blood* **2005**, *106*, 996.
22. (a) Vanotti, E.; Caldarelli, M.; Cirla, A.; Forte, B.; Ermoli, A.; Menichincheri, M.; Pillan, A.; Scolaro, A. WO2007/110344, **2007**; (b) Brasca, M. G.; Bandiera, T.; Bertrand, J. A.; Gnocchi, P.; Mirizzi, D.; Nesi, M.; Panzeri, A. WO2012/143248, **2012**.
23. Vanotti, E.; Amici, R.; Bargiotti, A.; Berthelsen, J.; Bosotti, R.; Ciavolella, A.; Cirla, A.; Cristiani, C.; D'Alessio, R.; Forte, B.; Isacchi, A.; Martina, K.; Menichincheri, M.; Molinari, A.; Montagnoli, A.; Orsini, P.; Pillan, A.; Roletto, F.; Scolaro, A.; Tibolla, M.; Valsasina, B.; Varasi, M.; Volpi, D.; Santocanale, C. *J. Med. Chem.* **2008**, *51*, 487.
24. Menichincheri, M.; Albanese, C.; Alli, C.; Ballinari, D.; Bargiotti, A.; Caldarelli, M.; Ciavolella, A.; Cirla, A.; Colombo, M.; Colotta, F.; Croci, V.; D'Alessio, R.; D'Anello, M.; Ermoli, A.; Fiorentini, F.; Forte, B.; Galvani, A.; Giordano, P.; Isacchi, A.; Martina, K.; Molinari, A.; Moll, J. K.; Montagnoli, A.; Orsini, P.; Orzi, F.; Pesenti, E.; Pillan, A.; Roletto, F.; Scolaro, A.; Tato', M.; Tibolla, M.; Valsasina, B.; Varasi, M.; Vianello, P.; Volpi, D.; Santocanale, C.; Vanotti, E. *J. Med. Chem.* **2010**, *53*, 7296.
25. Uozumi, K.; Otsuka, M.; Ohno, N.; Moriyama, T.; Suzuki, S.; Shimotakahara, S.; Matsumura, I.; Hanada, S.; Arima, T. *Leukemia* **2000**, *14*, 142.
26. Di Noto, R.; Pane, F.; Camera, A.; Luciano, L.; Barone, M.; Lo Pardo, C.; Boccuni, P.; Intrieri, M.; Izzo, B.; Villa, M. R.; Macrí, M.; Rotoli, B.; Sacchetti, L.; Salvatore, F.; Del Vecchio, L. *Leukemia* **2001**, *15*, 1641.
27. Davis, M. I.; Hunt, J. P.; Herrgard, S.; Ciceri, P.; Wodicka, L. M.; Pallares, G.; Hocker, M.; Treiber, D. K.; Zarrinkar, P. P. *Nat. Biotechnol.* **2011**, *29*, 1046.
28. Colombo, M.; Riccardi-Sirtori, F.; Rizzo, V. *Rapid Commun. Mass Spectrom.* **2004**, *18*, 511.
29. Otwinowski, Z.; Minor, W. *Methods Enzymol.* **1997**, *276*, 307.
30. McCoy, A. J.; Grosse-Kunstleve, R. W.; Adams, P. D.; Winn, M. D.; Storoni, L. C.; Read, R. *J. Appl. Crystallogr.* **2007**, *40*, 658.
31. Emsley, P.; Cowtan, K. *Acta Crystallogr. D Biol. Crystallogr.* **2004**, *60*, 2126.
32. Murshudov, G. N.; Vagin, A. A.; Dodson, E. J. *Acta Crystallogr. D Biol. Crystallogr.* **1997**, *53*, 240.
33. Felder, E. R.; Badari, A.; Disingrini, T.; Mantegani, S.; Orrenius, C.; Avanzi, N.; Isacchi, A.; Salom, B. *Mol. Diversity* **2012**, *16*, 27.
34. Pevarello, P.; Brasca, M. G.; Amici, R.; Orsini, P.; Traquandi, G.; Corti, L.; Piutti, C.; Sansonna, P.; Villa, M.; Pierce, B. S.; Pulici, M.; Giordano, P.; Martina, K.; Fritzen, E. L.; Nugent, R. A.; Casale, E.; Cameron, A.; Ciomei, M.; Roletto, F.; Isacchi, A.; Fogliatto, G.; Pesenti, E.; Pastori, W.; Marsiglio, A.; Leach, K. L.; Clare, P. M.; Fiorentini, F.; Varasi, M.; Vulpetti, A.; Warpehoski, M. A. *J. Med. Chem.* **2004**, *47*, 3367.